ISTANBUL TECHNICAL UNIVERSITY ★ GRADUATE SCHOOL OF SCIENCE ENGINEERING AND TECHNOLOGY

ACTIVATED CARBON NANO-FIBER FROM POLYMERS

M.Sc. THESIS

Sahand FARAJI

Department of Chemical Engineering

Chemical Engineering Programme

MAY 2014

ISTANBUL TECHNICAL UNIVERSITY ★ GRADUATE SCHOOL OF SCIENCE ENGINEERING AND TECHNOLOGY

ACTIVATED CARBON NANO-FIBER FROM POLYMERS

M.Sc. THESIS

Sahand FARAJI
(506121028)

Department of Chemical Engineering

Chamical Engineering Programme

Thesis Advisor: Prof. Dr. M. Ferhat YARDIM

MAY 2014

İSTANBUL TEKNİK ÜNİVERSİTESİ ★ FEN BİLİMLERİ ENSTİTÜSÜ

POLİMERLERDEN AKTİF KARBON NANO-FİBER OLUŞTURMA

YÜKSEK LİSANS TEZİ

Sahand FARAJI
(506121028)

Kimya Mühendisliği Anabilim Dalı

Kimya Mühendisliği Programı

Tez Danışmanı: Prof. Dr. M. Ferhat YARDIM

MAYIS 2014

Sahand-Faraji, a **M.Sc.** student of ITU Institute of **Science Engineering and Technology** student ID 506121028, successfully defended the **thesis** entitled "**ACTIVATED CARBON NANO-FIBER FROM POLYMERS**", which he prepared after fulfilling the requirements specified in the associated legislations, before the jury whose signatures are below.

Thesis Advisor :	**Prof. Dr. M. Ferhat YARDIM** İstanbul Technical University	.....
Jury Members :	**Prof. Dr. M. Ferhat YARDIM** İstanbul Technical University	.....
	Prof. Dr. Yuda YÜRÜM Sabanci University	.....
	Prof. Dr. Ahmet SİRKECİOĞLU İstanbul Technical University	.....

Date of Submission : 05 May 2014
Date of Defense : 16 July 2014

To whom I love,

FOREWORD

First of all, I would like to express my sincere gratitude to my advisor Prof. Dr. M. Ferhat Yardim for his guidance throughout my graduate study. It has been my honor to work with him. During the past two years, he provided me with comfortable environment for research, so that I can fulfill my thoughts without many restrictions. Besides, his words and actions improved my personality features. I am grateful to him for being a great mentor in both scientific and extracurricular aspects.

I also wish to thank Prof. Dr. Sezai Sarac, for his valuable guidance, support, feedback and insightful criticism during my research. Also Prof. Dr. Ahmet Sirkecioglu offer me great convenience in using the equipments in the labs.

I would like to give my thanks to members of Electropolymerization and Nanotechnology Laboratory Research Group, specially MSc Dilek Suadiye for her sincere help.

I would also like to give special thanks to my friend MSc Sina Sadighikia for his sincere and genuine help with SEM analysis and also thank to MSc Ozlem Haval Demirel for her help with ASAP analysis.

I express my gratitude to my friends MSc İrem Tunç and MSc Houman Bahmani Jalali for helping me in writing turkish summary.

Special thanks to PhD Ahmet Halil Avci for his help with FTIR and TGA analysis and helping me dealing the obstacles I have faced during the experiments. Also thank to MSc Halil Balci for his moral supports.

I want to thank to my best friends MSc Babak Vajdi and MSc Behnam Sadri for their support, help, patience and friendship. They were with me whenever I needed, no matter how much distance there was between us.

Appriciation extended to all of my friends eighter in Istanbul or other places all over the world. With them I was never alone even at the hardest times through this work.

Most of all, I would like to express my never ending love to my mother Roghayeh Rismani, my father Eltefat Faraji and my sister Sanaz Faraji for their unconditional supports and care during my whole life and finally my girlfriend Mina Deljavan for her great kindness, chastity, patience, affection and being my motivation.

May 2014

Sahand FARAJI
(Chemical Engineer)

TABLE OF CONTENTS

Page

ABBREVIATIONS

ASAP	**:** Accelerated Surface Area and Porosimetry System
AC	**:** Activated Carbon
ACF	**:** Activated Carbon Fiber
ACNF	**:** Activated Carbon Fiber
AN	**:** Acrylonitrile
APS	**:** Amonium persulphate
CF	**:** Carbon Fiber
CNF	**:** Carbon nanoFiber
C2H0	**:** Electrospun Poly(acrylonitrile-co- itaconic acid)(85:15)%Wt.
C2S	**:** Stabilized Poly(acrylonitrile-co- itaconic acid)(85:15)%Wt.
C2Ca	**:** Carbonized Poly(acrylonitrile-co- itaconic acid)(85:15)%Wt.
C2Act	**:** Activated Poly(acrylonitrile-co- itaconic acid)(85:15)%Wt
C4H0	**:** Electrospun Poly(acrylonitrile-co-vinyl acetate)(85:15)%Wt.
C4S	**:** Stabilized Poly(acrylonitrile-co-vinyl acetate)(85:15)%Wt.
C4Ca	**:** Carbonized Poly(acrylonitrile-co-vinyl acetate)(85:15)%Wt.
C4Act	**:** Activated Poly(acrylonitrile-co-vinyl acetate)(85:15)%Wt.
DMF	**:** Dimethylformamide
FTIR	**:** Fourier Transform Infrared Spectroscopy
IA	**:** Itaconic acid
PAN	**:** Poly acrylonitrile
P(AN-Co-IA)	**:** Poly(acrylonitrile-co-itaconic acid)
P(AN-Co-VAc)	**:** Poly(acrylonitrile-co-vinyl acetate)
P0H0	**:** Electrospun Acrylonitrile homopolymer.
P0S	**:** Stabilized Acrylonitrile homopolymer
P0Ca	**:** Carbonized Acrylonitrile homopolymer
P0Act	**:** Activated Acrylonitrile homopolymer
SEM	**:** Scanning Electron Microscope
TGA	**:** Thermal Gravimetric Analysis
VAc	**:** Vinyl Acetate

LIST OF TABLES

Page

LIST OF FIGURES

Page

ACTIVATED CARBON NANO-FIBER FROM POLYMERS

SUMMARY

Because of carbon nano fibers and ACNFs vast application area, such as aeroscape, civil and tissue engineering, biotechnology, batteries and environmental, it became an important research interest of scientist lately. Nanaoscale materials have a great interest due to their exceptional properties. Carbon nanomaterials such as carbon nanofibers, carbon nanotubes and carbon nanowires are provide fascinating field of study for reasercher in last few decades. Depends on carbon fibers applications, the precursors could be chosen from different materials. Nowadays PAN based carbon fibers and ACNFs are most considered by researchers because of its chemical structure and subsequently its unique and proper behaviour when applied to a activation process heat treatment. PAN homopolymer should be the optimal choice to produce PAN fibers, but it hindered the alignment of molecule chain during spinning, which resulted in poor quality of carbon fiber. Electrospinning with copolymers offers property enhancement of polymeric materials, including modifying of thermal stability, mechanical strength and barrier properties, and has therefore been often pursued for engineering structural applications. So selection of a suitable comonomer is an important step.

In the present study, three different polymers such as AN homopolymer, P(AN-co-IA) and P(AN-co-VAc) copolymers used as precursor to provide activated carbon nano fibers.

Electrospinning method which is the most well-known method to produced the fibers in the nano scales used to produced the desired nano fibers. These fibers exposed under a specific heating regim to became activated carbon nano-fibers from different precursors.

Electrospun samples stabilized and carbonized and then consequently activated by CO_2. Nanofibers which processed under the heat-treatment conditions were characterized by means of weight loss measurement, thermogravimentric analysis (TGA), scanning electron microscopy (SEM), porosity and surface area analysis (ASAP) and finally attenuated total reflection-Fourier transform infrared spectroscopy (ATR-FTIR). The fibers diameter recorded by image proccessing of SEM images.

Those mentioned above analysis carried out on precursors in the all steps of activation process(oxidative stabilization, carbonization and activation) and evaluated the effect of using copolymers in compare with homopolymer.

The aim of these work is enhance thermal stability of PAN based CNFs and ACNFs by using copolymers instead of acrylonitrile homopolymer.

After completing cyclization reaction and interchain polymerization of nitrile groups, PAN fiber decomposes at 295 °C. The homopolymer of AN showed the main thermal decomposition at about the mentioned temperature (295 °C). However, for compolymers which contained VAc thermal decomposition temperature was about 315°C and this themperature for P(AN-co-IA) copolymer was about 305 °C.

For Acrylonitrile homopolymer, as-electrospun fibers diameter was about 610 nm while during the specific heat treatment, after stabilization the fibers diameter drop to 580 nm and diameters for carbonized and activated form of fiber are about 450 and 350 nm respectively. As mentioned before, decreasing the fiber diameter was due to the shirinkage that result of evolving gases (burn off) occurring at high temperatures used during carbonization and activation.

The diameter value for P(AN-co-IA) in as-electrospun, oxidative stabilized, carbonized and activated fibers was about 510, 485, 345 and 440 nm respectively. However these values for P(AN-co-VAc) were 470, 355, 320 and 350 nm for as-electrospun, stabilized, carbonized and activated fibers.

Total pore volume was increased same as the result of BET specific surface area, comparing with electrospun fibers and activated fibers from 0.67 to 260 m^2/g about 400 times for acrylonitrile homopolymer fibers. BET surface area values for electrospun fibers augmented after activation form 3.46 to 375 m^2/g (about 110 times) and from 0.09 to 408 m^2/g (about 4500 time) for P(AN-co-IA) and P(AN-co-VAc) copolymers respectively. It demonstrated the gigantic effect of heating regim and activation process on the BET specific surface area of the fiber which deriven from acrylonitrile and vinyl acetate copolymers that could change 4500 time after the specific heat treatment.

The synthesized AN homopolymer, P(AN-co-VAc) and P(AN-co-IA) copolymers are characterized spectroscopically by FTIR-ATR. PAN shows its characteristic absorption peaks at 2243 cm^{-1} and 1451 cm^{-1}, corresponding to CN stretching and CH bending, respectively.

As a result, thermal stability improved by using P(AN-co-IA) and P(AN-co-VAc) copolymers instead of homopolymer of acrylo nitrile as precursor of CNFs and also ACNFs.

POLİMERLERDEN AKTİF KARBON NANO-FİBER OLUŞTURMA

ÖZET

Yaygın olarak kullanılan endüstriyel adsorbanlar arasında çevre kirliliğini kontrol amacıyla, şu anda kullanılan adsorbanların en önemlisi, yüksek gözenekliliğe sahip aktif karbonlardır. Ticari olarak aktif karbonlar, odun, turba, linyit, kömür, mangal kömürü, kemik, Hindistan cevizi kabuğu, pirinç kabuğu, fındık kabuğu ve yağ ürünlerinden elde edilen karbonların çeşitli işlemlerden geçirilerek aktive edilmesiyle elde edilirler.

1900' lü yılların başında, şu anki aktif karbon üretiminin temelini oluşturan patentler yayınlanmıştır. Bu patentler, bugün bile hala geçerli olan aktif karbon üretiminin iki temel prensibini açıklamaktadır. Bunlar kimyasal aktivasyon ve gaz aktivasyonudur. 1920 yılından sonra, ilk olarak, aktif kömür su arıtılmasında kullanılmaya başlanmış, fakat yaygın bir kullanım sağlanamamıştır. Ancak, 1927 yılında Almanya'da içme suyundaki klorofenol kokusu büyük problem yarattığından, şehir suyunun hazırlanması sırasında aktif karbon kullanımı da büyük önem kazanmıştır.

Aktif karbon, 1929 yılında Hamm Water Works'da granüler formda, bundan bağımsız olarak 1930'da Harrison tarafından Michigan Bay City'de, yine 1929 yılında Spalding tarafından içme suyundaki kokuların uzaklaştırılması amacıyla toz halinde kullanılmıştır. 1932 yılına gelindiğinde Amerika'da 400 fabrika, 1943 yılında ise yaklaşık 1200 fabrika istenmeyen kokuların kontrolünde aktif karbonu kullanmıştır.

Aktif karbon, büyük kristal formu ve oldukça geniş iç gözenek yapısı ile karbonlu adsorbanlar ailesini tanımlamada kullanılan genel bir terimdir. Aktif karbonlar, insan sağlığına zararsız, kullanışlı ürünler olup, oldukça yüksek bir gözenekliliğe ve iç yüzey alanına sahiptirler .Aktif karbonlar, çözeltideki molekül ve iyonları gözenekleri vasıtasıyla iç yüzeylerine doğru çekebilirler ve bu yüzden adsorban olarak adlandırılırlar.

Nano lifler, genel olarak bir mikrondan daha düşük çapa sahip olan lifler olarak tanımlanmaktadır. Nano liflerden oluşan yüksek yüzey alanına sahip ve gözenekli yüzeyler, farklı özellikleri sebebiyle pek çok alanda kullanım olanağına sahip olmaktadırlar. Bu çalışmada, farklı polimerden oluşturulmuş karbon nano liflerin üretim yöntemleri, termal özellikleri ve kullanım olanakları ile ilgili bilgiler verilmektedir.

Karbon nanolif ve ACFN lerin havacılık, inşaat, doku mühendisliği, biyoteknoloji, pil, çevre mühendisliğindeki kullanımlarından dolayı bugünlerde bilim adamlarının en önemli araştırma konularından biri olarak yerini almıştır.

Nano boyutlarındaki malzemeler kendilerine has ve özel özelliklerinden dolayı göz önündedirler. Son yıllarda Karbon nano lif, Karbon nanotüp, Karbon nanotel gibi

Karbon köklü nano malzemeler en önemli araştırma konulardan biri olmuştur. Karbon nano lifler uygulamalarına göre uygun maddelerden üretilirler.

Bugünlerde PAN köklü ve ACFN nano lifler kendilerine özel yapıları ve ısı işlemlerinden sonra gösterdikleri özel tavırdan dolayı araştırmacıların bir numara tercihi olmuştur. PAN homopolimerler Karbon nanoliflerin üretimi için en uygun malzemedir ama yollaştığı sorunlardan dolayı karbon lifin kalitesini düşürüyor. Copolimerle Elektrospinleme uygulaması polimerlerin termal, mekanik ve bariyer özelliklerini iyileştirip geliştiriyor, dolayısıyla uygulama yönünde araştırmacıların en önemli kavramlarından biri olmuştur. Bu esnada comonomer seçimi en hassas ve önemli konudur.

Bu çalışmada, AN homopolymer, P(AN-co-IA) ve P(AN-co-VAc) gibi üç faklı copolimer aktivleşmiş karbon lifi üretimi için kullanılmıştır.

Lif üretimi için en önemli ve pratik yöntem olan elektrospin yöntemi kullanılmıştır. Değişik malzemelerden üretilen lifler değişik ısı işlemlerinden geçerek aktifleşmişlerdir.

Elektrospinlenmiş lifler stabilize edildikten sonra karbonize edilip ve en sonda da CO_2 ile aktifleşmiştir. Üretilmiş lifler ısı işlemlerinden sonra TGA, SEM, ASAP, FT-IR testlerinden geçmiştir. Lif çapları SEM resimleriyle hesaplanmıştır.

Aktif karbonun iç yüzeyi(aktifleştirilmiş yüzey) çoğunlukla BET yüzeyi olarak (m^2/g) ifade edilir. Yüzey alanı azot (N_2) gazı kullanılarak ölçülür. Kirlilik oluşturan maddeler, aktif karbonun yüzeyinde tutulacağından, yüzey alanının büyüklüğü kirliliklerin giderilmesinde oldukça etkili bir faktördür.

Prensip olarak, yüzey alanı ne kadar büyükse, adsorpsiyon merkezlerinin sayısının da o kadar büyük olduğu düşünülür

Yukarıda belirtilmiş testler tüm steplerde(oxidative stabilization, carbonization and activation) alıtmıştır ve copolimer kullanmanın etkisi homopolimer kullanma ile kıyaslanmıştır.

Bu çalışmanın amacı acrylonitrile homopolymer yerine copolimer kullanmakla PAN ve ACNF köklü karbon nano lifler termal stablizasyonunu artırmaktır.

Halkalaşma reaksiyonu tamamlandıktan ve nitril gruplarının polimerizasyonundan sonra, PAN fiber 295 ˚C'de bozunmaktadır. AN homopolimeri, söz konusu sıcaklık olan 295 ˚C'de ana termal bozunmanın gerçekleştiğini göstermektedir. Fakat VAc içeren kopolimerlerin termal bozunma sıcaklığı yaklaşık 315 ˚C iken, P(AN-co-IA) kopolimerleri için bu sıcaklık yaklaşık 305 ˚C'dir.

Akrilonitril homopolimerler için özgül ısıl işlem boyunca fiberlerin çapı 610 nm iken, denge sağlandıktan sonra fiberlerin çapı 580 nm'ye düşmekte ve karbonize fiber ile aktif formdaki fiberin çapları sırasıyla 450 nm ve 350 nm olmaktadır. Daha önceden de belirtildiği üzere karbonizasyon ve aktivasyon sırasında kullanılan yüksek sıcaklıkta oluşan yanma gazları sonucunda oluşan büzüşmeden dolayı fiberlerin çapı azalmıştır.

P(AN-co-IA)'nın as-electrospun fiberde, kararlı durumdaki fiberde, karbonize fiberde ve aktive fiberdeki çap değerleri yaklaşık olarak sırasıyla 510, 485, 345 ve 440 nm iken P(AN-co-VAc) için 470, 355, 320 ve 350 nm'dir. (bulunmuştur).

Electrospun akrilonitril homopolimer bazlı fiberlerde BET yüzey alanı 0.67 m^2/g iken, aktive olduktan sonra bu değer 260 m^2/g'a yükselmiştir. Bu oranda BET yüzey

alanının yaklaşık 400 kat arttığını göstermektedir. Aktivasyon formundan sonra electrospun fiberler için BET yüzey alanı değeri, P(AN-co-IA) için 3.46'dan 375 m^2/g'a (yaklaşık 110 kat), P(AN-co-VAc) için ise 0.09'dan 408 m^2/g'a (yaklaşık 4500 kat) artmıştır.

Aktivasyon prosesi ve ısı rejiminden oldukça etkilenen Akrilonitril ve vinil asetat kopolimerlerinden türeyen fiberin BET yüzey alanı özgül ısıl işleminden sonra 4500 kat artmıştır.

Sentezlenen AN homopolimer, P(AN-co-VAc) ve P(AN-co-IA) kopolimerlerinin karakterizasyonu FTIR-ATR kullanılarak gerçekleştirilmiştir.

CN stretching ve CH bending'den dolayı, PAN'ın karakteristik absorbsiyon pikleri 2243 cm^{-1} ve 1451 cm^{-1}, olarak görünmüştür.

Akrilonitril kopolimerleri ön-maddelerden yapılan nano-elyaflar akrilonitril homopolimerler ön-maddelerden yapılan nano-elyaflarla karşılaştırdıkta daha iyi bir termal stabiliti göstermektedir.

1. INTRODUCTION

For almost a century, the long life members of the family of carbon materials, the giants of the industry as it were, i. e. graphites, synthetic graphites, delayed cokes, activated carbons, and carbon blacks have all undergone a continuous process of renovation and improvement. But that is not all: the search for new, novel, different forms of carbon never ceases. The success story for new materials must be awarded to the polyacrylonitrile fiber in the development of which William Watt, in the United Kingdom, played a significant role. The carbon fiber story actually belongs to the last century starting with the invention of the electric light bulb. The continuous improvement in the mechanical properties during to last two decades of these PAN has meant that the mesophase-type of fiber has not been sold competitively against PAN.

Carbon filaments or whiskers, smaller in dimensions than the fiber, and generated from carbon growing on metal particles offer another new form of carbon. They can be grown on normal fiber systems so giving a higher density composite, or form a composite in their own right. They are comparatively quite graphitic and being hollow offer enhanced surface accessibility. Their future must be watched carefully. Still in the area of fibers, there are the activated, microporous carbon fibers. This material offer flexibility in terms of presentation to the adsorbate, e.g. as a cloth, or in frames for liquid purification, etc. Initial incentives were the protection of military personnel and equipment in scenarios of chemical warfare. Other, domestic markets must be established.

PAN fibers are not only that have exotic uses as in aircraft or possible space stations. A pitch-based fiber is also on the market. It is made of stabilized petroleum pitch and finds various applications such as a building material, a concrete reinforcement, in solar collection cells, brake and clutch friction materials, static dispersions, thermal and sound insulator and in electrical conductors.

1.1 Literature Review

Carbon fibers can be prepared from polymeric precursor materials such as polyacrylonitrile (PAN), cellulose, pitch and polyvinylchloride, which are discussed in detail later. PANbased carbon fibers predominate and have good strength and modulus properties, whereas carbon fiber can be made with a higher modulus, although a lower strength, using a pitch-based precursor. Fibers from Rayon and similar materials are also used but no longer produced in quantity [1]. Mechanical and structural characterization such as bending modulus and stress failure of individual carbonized of electro spun PAN-derived nanofibers presented by E. Zussman et al. Comparing the mechanical properties of the electrospun PAN-derived carbon nanofibers to commercial PAN-derived carbon fibers is of interest. Besides the size effect (the diameter of commercial fibers is greater than 5 μm), the commercial carbonized fibers are usually produced from copolymers (e.g., 10% methyl methacrylate), subjected to post-drawing processes with heating under tension, and carbonized at between 1400 and 1700 ˚C). However electrospun PAN-derived carbon nanofibers fabricated that were then carbonized, with diameters ranging from 50 to 250 nm. After the carbonization process the average diameter shrank to 50% of as-electrospun fibers.The stiffness and strength of those discussed here are lower than commercial PAN-based fibers. If the polymer precursor morphology and molecular orientation, along with the carbonization process, can be optimized it is possible that the stiffness and fracture strength of carbon nanofibers based on the electrospinning process could be substantially improved [2].

PAN homopolymer should be the optimal choice to produce PAN fibers, but it hindered the alignment of molecule chain during spinning, which resulted in poor quality of carbon fiber. So selection of a suitable comonomer is an important step, which has been a main subject of the study that Xiang et al. done on characterization of copolymerization of acrylonitrile with four comonomers including itaconic acid, acrylamide, methyl acrylate and ammonium salt of itaconic acid in dimethyl sulfoxide solvent and suitable copolymers for carbon fibers. mechanical properties of the resultant carbon fibers developed for AN/IA system are the best [3].

As an application point of view for PAN carbon fibers, the membranes which based on PAN CFs can be successfully pyrolyzed into carbon membrane using nitrogen gas pyrolysis system. Pyrolysis temperature influences the resultant carbon membrane by

altering the structure and pore properties of the membrane. FTIR results concluded that the carbon yield still could be increased by pyrolyzing PAN membranes at temperatures higher than 800 °C because of the existence of other functional group instead of CH group. Gas adsorption analysis showed that the average pore diameter increased up to 800 °C. This result encourages further research on higher pyrolysis temperature since it has been hypothesized that the pore diameter will shrink at relatively higher temperature [4].

Free radical copolymerization of acrylonitrile (AN)–vinyl acetate (VAc) was performed for five different feed ratio of VAc (wt %) by using ammonium persulfate in the aqueous medium. The effect of VAc content on the spectrophotometric and thermal properties of AN-VAc copolymers was investigated by FTIR, DSC and TGA. also the morphologic properties of nano fibers was studied by SEM and AFM.The average nanofiber diameter in 10(wt%) is 445nm however this value shranked to 130 nm by increasing the feed ratio to 40(wt%). TGA study presented that by increasing the feed ratio of VAc from 10 to 50 wt %, the thermal decomposition temperatures were increased from 306°C to 343°C. These values are all higher than that of homopolymer of AN, indicating that thermal stability of PAN is improved after being copolymerized with VAc, and thus con- firming the effect of VAc functional groups existed in P(AN-co- VAc) in addition to nitrile groups of PAN [5]. Synthesis of P(VAc-AN) and derivatized water-soluble of these copolymes and also experiments on the copolymerization of vinyl acetate with eight representative monomers presented studied by researchers[6, 7]. Fabricating P(VAc-AN) composite films by chemical polymerization of pyrrole with cerium(IV) and FTIR spectroscopic study on the effect of amount od pyrrole and temperature on the composite film properties carried out by Cetiner et al.[8]. The vast range application of these composit in the previous works of researcher inspire a new study on the P(VAc-AN) based carbon nano fibers.

characterization of PAN based nanofibers microstructural, electrical, and mechanical properties also investigated several carbonization procedures by varying final carbonization temperatures in the range from 1000 to 2200 °C with increase of the final carbonization temperature, the carbon nanofibers became more graphitic and structurally ordered the carbon nanofiber bundles possessed anisotropic electrical conductivities, and the differences between the parallel and perpendicular directions to the bundle axes were over 20 times, This was because the carbon nanofibers in the

bundles only had occasional contacts with neighboring nanofibers, despite some did entangle with others; the tensile strengths and Young's moduli of the prepared carbon nanofiber bundles were in the ranges of 300–600MPa and 40–60 GPa, respectively. PAN electro spun fibers carbonized in two different temperature [9]. Also. Pashaloo et al. reported the fabrication and characterization of polyacrylonitril (PAN) nanofibers by electrospinning and further development of the as-spun PAN nanofibers into carbon nanofibers by changing the carbonization temperature between 800°C and 1000°C. Morphologies, structures and thermal properties of PAN, stabilized and carbonized nanofibers were investigated by (SEM), (FTIR) and (TGA). Nanofibers with diameter ranging from 180 to 640 nm were obtained by electrospinning of PAN/DMF solution. The average diameter of the stabilized PAN nanofibers appeared to be almost the same as that of the as-electrospun nanofibers, while the average diameters of the carbonized PAN nanofibers were significantly reduced. The oxidative stabilization at 290ºC and 2 h of PAN precursors during their conversion to carbon nanofibers is a time-consuming process and plays an important role in determining the final structure and mechanical properties of resultant fibers [10, 11].

1.1.1 Oxidative Stabilization of Carbon Fibers and Nano-Fibers

In the heat treatment processes which convert PAN fiber to carbon fiber, the most essential process is the stabilization or oxidation step. The main purpose of this step is to cross-link PAN chains and prepares a structure that can withstand the rigors of high temperature processing [12–16]. The stabilization is intended to prevent melting or fusion of the fiber, to avoid excessive volatization of elemental carbon in the subsequent carbonization step and thereby to maximize the ultimate carbon yield from the fiber precursor [12, 16, 17]. The chemistry of the stabilization process is complex, but generally consists of cyclization of the nitrile groups (C≡N) and crosslinking of the chain molecules in the form of –C=N–C=N– [14, 16]. Houtz[18] proposed the simplest fully aromatic cyclized structure for PAN homopolymer without considering the presence of oxygen during stabilization as shown in **Table 1.1**, reaction (i). Based on the cyclization structure postulated by Houtz [18], later on, numerous researchers proposed other alternative structures as shown in **Table 1.1** (ii), (iii) and (iv)[19–21] . Standage and Matkowsky represented an oxidized structure with epoxide bridges type bonding to cyclized PAN [19]. Meanwhile, Friedlander et al. [20] proposed another structure which suggested that the PAN molecules were actually able to absorb oxygen

rapidly but not completely in order to form polynitrone (–C=N(→O)–)n units. While Watt and Johnson [21] proposed a ladder structure with ketonic oxygen on the cyclized structure of PAN.

Table 1.1: Stabilization reaction mechanism of PAN homopolymer.

I.	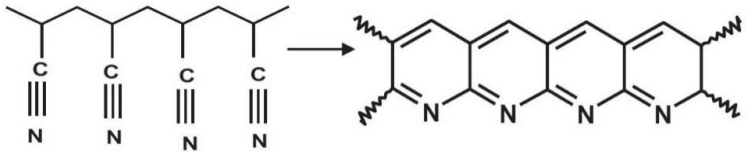	Houtz[18]
II.	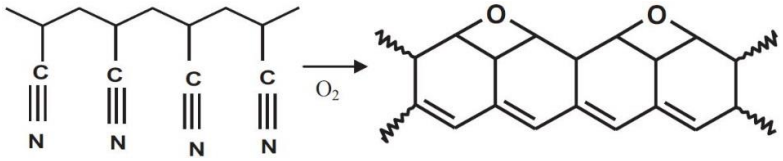	Standage and Matkowsky[19]
III.	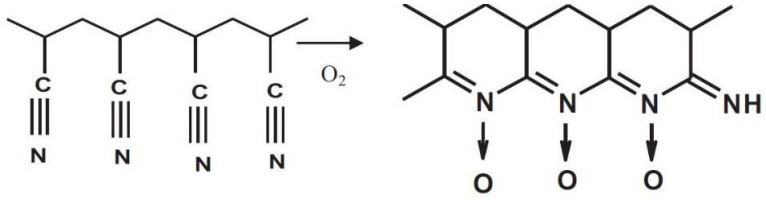	Friedlander et al.[20] Grassie et al.[22] Burlant and Parsons [23] LaCombe[24]
IV.	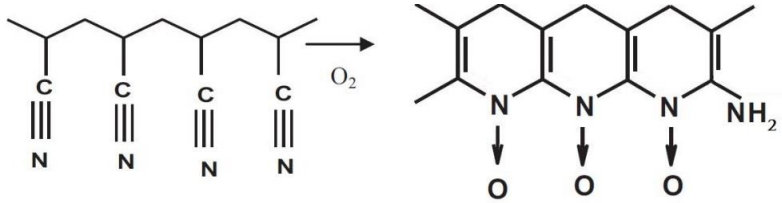	Coleman and Petcavich[25] Fochler et al.[26] Xue et al.[27]
V.	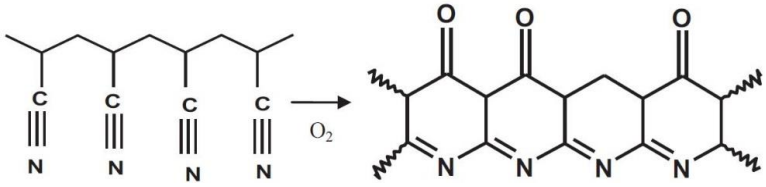	Watt and Johnson[21]

1.1.2 Role of Comonomers in Stabilization

The use of comonomers partially disrupted the nitrile–nitrile interactions of PAN, allowing for better chain alignment and acting as an initiator in the formation of the ladder polymer [13, 28–30]. Figure 1.1 shows cyclization reaction in PAN-itaconic acid (IA) initiated through an ionic mechanism [29]. The Fourier transform infrared

spectroscopy (FTIR) analysis by Ouyang et al. [30]indicated that the cyclization of nitrile groups was initiated at a lower temperature by the IA comonomer and the stabilization proceeded at a more moderate pace in P(AN-IA) than in PAN homopolymer. These ionic cyclization reactions also showed a kinetic advantage at low temperature over other oxidative stabilization reactions in air atmosphere [28, 30].

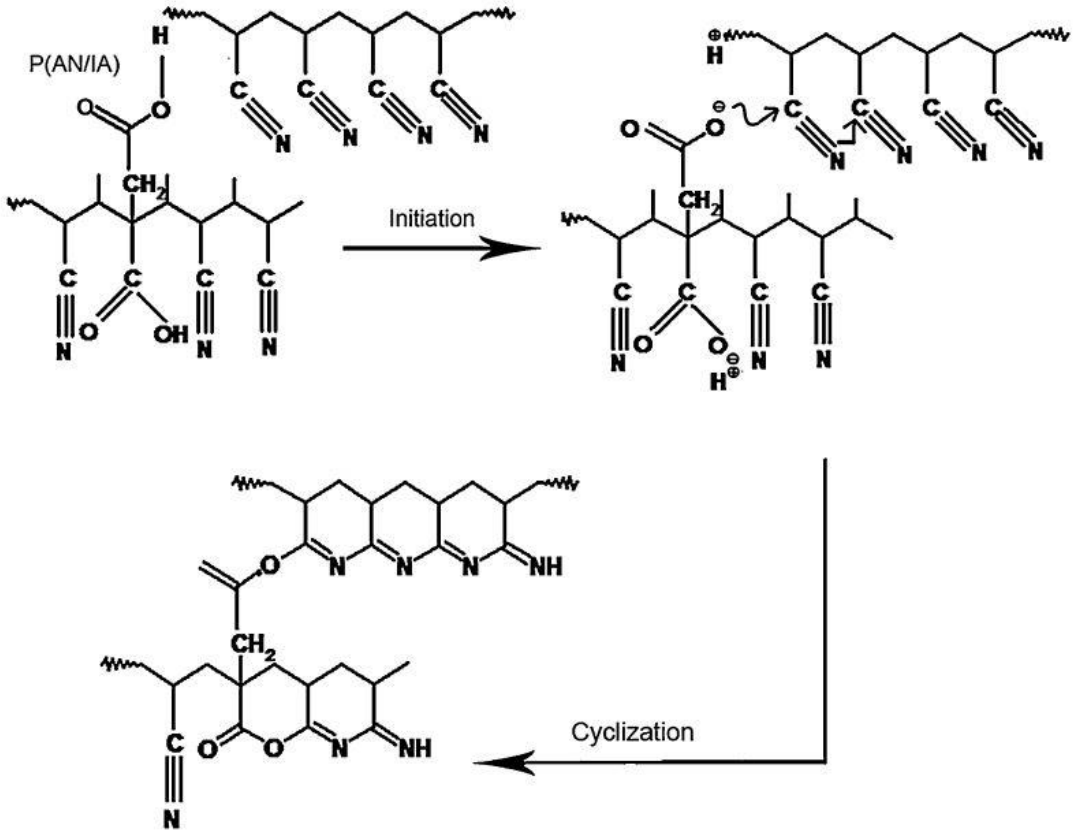

Figure 1.1: Cyclization in PAN-itaconic acid (IA) initiated through an ionic mechanism[29].

1.1.3 Influences of process variables during oxidative stabilization

Table 1.2 lists several important parameters and their optimum conditions during oxidative stabilization done by previous researchers. It can be concluded that the stabilization process is greatly influenced by several variables such as the pyrolysis temperature[31–33] and its heating rate [9], the tension of the fiber [34–36], total stabilization time and the dwell time[28, 36–38], air flowrate [17, 37]and also the prestabilization treatment [17, 38, 39]. The heating rate for oxidative stabilization is usually at the range of 1–2°C min^{-1} [17, 28, 32, 37] and should not be higher than 5◦C min^{-1} [38, 40].

The air is circulated in the furnace throughout stabilization to control heat and mass transfers [12]. The normal air flow rate during oxidative stabilization is in the range of 1–5 L min^{-1} [17, 28, 37, 38]. The air flow rate should not be too slow and should not be too rapid as it is closely related to the heat and mass transfer of the fiber. Heat treatment involved in stabilization of PAN fiber is frequently carried out in the range of 180–300°C [12, 37, 41, 42]. Fitzer et al. [43, 44] suggested that in producing best performance carbon fiber, the best stabilization temperature is 270◦C, while Chen and Harrison [17] recommended the optimum stabilization temperature is 230◦C.

Table 1.2: Oxidative stabilization regime in the literatue for PAN fibers.

Researcher	Oxidative stabilization temperature	Heating rate	Air flowrate
Chen and Harrison[17]	230°C	1°C.min^{-1}	4 L.min^{-1}
Zhang et al.[32]	200-400°C	2°C.min^{-1}	NA
Hou et al.[45]	300°C	5°C.min^{-1}	3 L.min^{-1}
Yu et al.[35, 36]	195-280°C	NA	NA
Gupta and Harrison[28]	200-500°C	1°C.min^{-1}	4 L.min^{-1}
Hou et al.[37]	200-280°C	2°C.min^{-1}	3 L.min^{-1}
Mathue et al.[38]	230°C	5°C.min^{-1}	1 L.min^{-1}
Wu et al.[46]	160-230°C	1°C.min^{-1}	NA
Ge et al.[41]	190-275°C	NA°C.min^{-1}	NA
He et al.[42]	190-270°C	NA°C.min^{-1}	NA
Fazlitdinova et al.[47]	245-290°C	NA	NA
Tavanai et al.[48]	230°C	1°C.min^{-1}	0.04 L.min^{-1}
Wang et al.[49]	280°C	1°C.min^{-1}	NA
Lee et al.[50]	270°C	0.5°C.min^{-1}	NA

Cho et al. provided two tables which are presented the chemical compositions measured for PAN precursor web, the stabilized webs, and the carbonized nanofiberwebs processed at different temperatures and heating rates between 240°C and 280°C and also summary of the weight losses occurred during various carbonization processes. Total weight loss increase from 2.19% in 240 °C to 65.14%

in 280 °C. Also stabilization temperature affected the weight loss in the carbonization process that more the stabilization temperature is more the weght loss in carbonization [43]. The effect of oxidation on the structural integrity of multiwalled carbon nanotubes through acidic and basic agents has been studied by Datsyuk et al. [51].

in 1985 Fitzer published the study on controlling the properties of PAN base carbon fibers by the heat treatment cycle during stabilization and carbonization [44]. It was found that shrinkage measurements during stabilization under time linear heating show the start and the end of the stabilization reaction. The optimum heating rate up to the starting temperature for a copolymer fibre with 6% methylaclate and 1% itaconic acid was found as 5˚C/min. After starting of the reaction the heating rate has to be reduced to a rate of 1˚C/min to exclude overheating of the fibre by the exothermic reaction. Differential termal analysis measurments had been used for study of the kinetics of cyclization and oxidation of PAN during the thermal treatment in air and nitrogen medium [40, 52]. A review of heating treatments such as stabilization carbonization and graphitization on PAN based fiber also written by Rahaman et al. [12].

1.1.4 Carbonization

Some workers have found that the presence of moisture in the oxidized PAN fibers can reduce the strength of the carbon fiber produced and dry the oxidized PAN fibers prior to entry into a low temperature furnace.

The low temperature furnace can best be described as a tar removal furnace and normally comprises a multizone electrically heated slot furnace, purged with N_2 to prevent entrance of air and providing sufficient N_2 flow to remove evolved tars and gases. The temperature in the furnace is gradually increased in the zones to a fmal temperature of about 950°C, a temperature above which the tars are decomposed leading to the deposition of a sooty product on the fiber, which causes the filaments to stick together and the carbon fiber properties to drop. Bromley and co-workers [53] at Harwell determined the gases evolved during carbonization from 200-1000°C (H_2O, CO_2, NH_3, HCN, H_2, high molecular weight compounds, CO and CH_4). Gas evolution is considerably enhanced if a thermal run-away occurs. Since the maximum temperature will be 1000°C, it is possible to use a high nickelalloy for the fabrication of the furnace muffle, but the alloy must be carefully chosen to provide adequate strength at operating temperatures and possess adequate resistance to internal and

external environments so that it does not corrode. Figure **1.2** illustrated the mechanisms fot the carbonization stages of PAN carbon fibers.

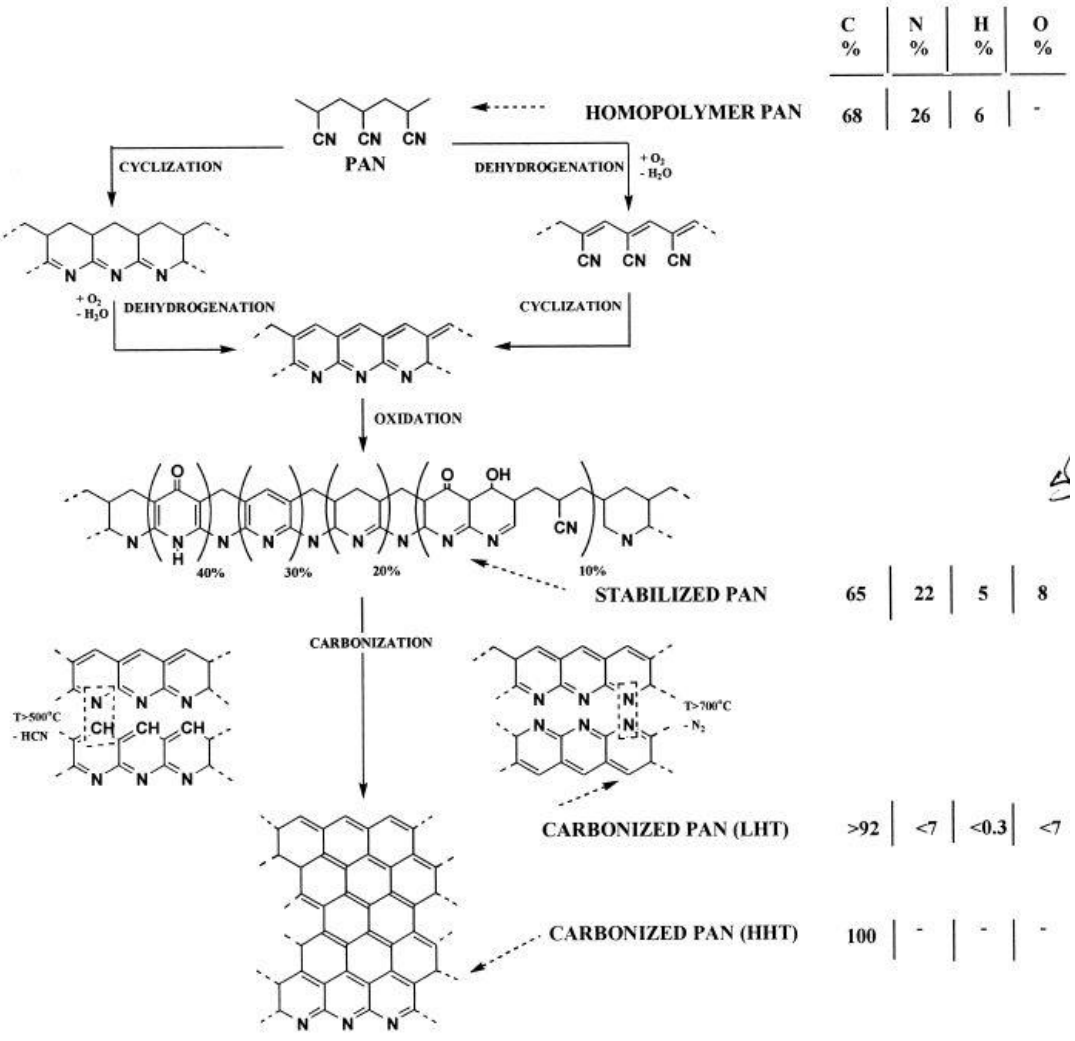

Figure 1.2: Mechanisms for the carbonization stages of PAN carbon fiber.

1.1.5 Activation

The commercial activated carbons on the market today are the result of continuous and intensive research and development toward optimization of application. The economics and availability of parent materials are as important as extents of available internal pore volumes (surface areas) associated with the right kind of porosity and surface chemistry. This means that a potential user of an active carbon should be as well familiar with the capabilities of his purchase as is the producer of the activated carbon. The availability of activated carbon for industrial use has much to do with accessing resources, renewing resources and processing to rigid specifications to control specific industrial applications. Only a handful of resources are used for

activated carbon production, including coals of several rank, peat as well as woods, fruit stones and nut- shells, as with coconut shells, as well as some synthetic organic polymers like PAN. Activated carbon is a member of a family of carbons ranging from carbon blacks to nuclear graphites, from carbon fibres and composites to electrode graphites, and many more. All come from organic parent sources but with different carbonization and manufacturing processes. These pyrolytic (deposited) carbons have a role in controlling the diameters of entrances to porosities of some activated carbons, and for the carbon-lithium battery [54].

Activation is selective gasification of carbon atoms (thermal activation) and activation involves the use of phosphoric acid (chemical activation) which is explained by detail in chapter 0. Activated carbon is porosity (space) enclosed by carbon atoms. Porosity of AC has the size of molecules and is probably slit-shaped. They are used for purification of water and of air and separation of gas mixtures. Emphatically ACs couldn't described as amorphous materials. In addition to shape and size of porosity of activated carbon materials the chemistry of surfaces of porosity (functionality) has also to be considered [55].

Activated carbon fiber (ACF) webs with a non-woven multi-scale texture in three different temperature were fabricated from polyacrylonitrile (PAN), and their characterizations was investigated by Wang et. al. The nanofibers in the ACF webs have a regular and flexuous fibrous morphology, of which the diameter becomes smaller as the activation temperature increases from 750 ˚C to 900 ˚C. The average diameter of the nanofibers was 800 nm, 363 nm and 285 nm for the ACF webs activated at 750 ˚C, 800 ˚C and 900 ˚C respectively. The shrinkage in diameter is due to the reactions during the thermal stabilization and the activation steps. ACF webs are prepared from electrospun PAN by air-oxidation stabilization and CO_2-activation at different temperatures. The as- made ACF webs have high specific surface area and a dual-mode pore size distribution, and feature a non-woven multi-scale texture, which endows it with excellent electrochemical performance. It has been found that higher activation temperature leads to higher capacitance and electrosorption capacity. The salt-removal tests in a CDI unit cell with electrodes made of ACF demonstrating that the ACF web electrodes made by electrospinning are of potential in electrochemical capacitive deionization for desalination of sea water [49].

Steam activated carbon nano fiber with electrospun PAN precursor prepared to be used as a highly efficient formaldehyde, a typical indoor pollutant adsorbent by Lee et al. The shallow and homoeneous microporous structure was attained by controlling the carbonization and steam activation conditions(i.e. activation period). The steam activation also made it possible to tune the nitrogen contents on ACNFs, which played a dominant role in the formaldehyde adsorption. Also the shallow microporosity of PAN-based ACNF was considered to provide preferential adsorption capability of formaldehyde even in the humid condition. In addition, the potential of the novel ACNFs in the practical application, that is, as amembrane fil- ter in forced-air-circulation-system was proved [50]. Kyotani presented a review work on the control of micro and mesoporosity. For the control of mesopores, many novel methods are proposed such as catalytic activation, polymer blend carbonization, organic gel carbonization and template carbonization. Also the time of activation parameter is play crucial role in the final BET surface area of metal doped ACNFs [56]. The effect of different chemical and thermal treatments to modification of surface chemistry of activated carbon studied by Figueiredo et al. [57]. Xiu and Li studied the ability of two activated carbon fibers to remove lead ions from aqueous solution using the breakthrough curve technique. The two carbons of the study were essentially similar as far as published analytical data were concerned, having surface areas of 976 and 993 m^2/g with basic functionalities of 0.287 and 0.419 mmol/g respectively. However, total pore volumes were somewhat different with values of 0.58 and 0.47 cm^2/g [58].

2. CARBON FIBER AND NANO-FIBERS

2.1 History of Carbon Fibers

The first carbon fibers made by Thomas Edison when he carbonized cotton thread to produce a filament for a light bulb in 1879. It was such an ineffectual effort and Edison finally substituted the fiber by a tungsten wire.

It wasn't until the late 1950′s that high tensile strength carbon fibers were discovered. Rayon became the first precursors used to create these modern fibers. Finally, it was replaced by more effective materials such as polyacrylonitrile (PAN) and pitch [59, 60].

2.2 Introduction to Carbon Fibers

Carbon fibers are used for reinforcing certain matrix materials to form composites. Carbon fibers contain 92% carbons in their composition. Carbon fiber composites can be short or continuous. The continuous carbon fibers composites are stronger than short carbon fibers. Commercial carbon fibers can be divided in three categories which are general-purpose, high performance and activated carbon fibers. The general purpose types have low tensile modulus, low tensile strength, isotropic and amorphous structure. The high performance carbon fibers have high strength and modulus. The activated carbon fibers have large number of open micro pores.

High performance carbon fibers composites, particularly those with polymer matrix, have became advantaged composite materials for aerospace, automobile, sporting goods and other applications due to their high strength, high modulus.

Commercial carbon fibers can be divided four main categories: Pitch, polyacrylonitrile (PAN), rayon and vapour grown carbon fibers. Making fibers from pitch have lower cost than from (PAN). The fabrication carbon fibers from pitch involve pyrolysis.

Pyrolysis is similar to charring, than forming carbon. Pyrolysis supplies higher carbon yield than (PAN) [61].

2.3 Propertieses of Carbon Fibers and Nano-Fibers

The manufacture and properties of carbon nanofibers are interesting because of the fibers' fascinating physical, thermal and chemical properties. Most of the past studies about CF and CNFs revolved around manipulating the properties for obtain a CNF with specific properties. To make the long story short, precise and concise of the carbon fibers properties which mentioned in the litetature, listed below [62–64]**:**

- Low density
- High tensile modules and strength
- Low thermal expansion coefficient
- Thermal stability in the absence of oxygen to over 3000^{o}C
- Excellent creep resistance
- Chemical stability, particularly in strong acids
- Biocompatibility
- High thermal conductivity
- Low electrical resistivity
- Availability in a continuous form
- Decreasing cost (versus time)

Disadvantages of carbon fibers include the following:

- Anisotropy
- Low strain to failure
- Compressive strength is low compared to tensile strength
- Tendency to be oxidized and became a gas upon heating in air above about 400^{o}C
- Oxidation of carbon fibers is catalyzed by an alkaline environment

Fitzer and co-workers showed that the concentration of reactive fiber surface groups on high modulus fiber is about one magnitude less than for high tenacity fiber, while wetting measurements and nitrogen determinations showed that the bond between fiber and matrix is at least 50% chemical in nature. The BET surface area of oxidized high tenacity fiber was about forty times that of high modulus fiber, suggesting that physical adhesion or mechanical interlocking was not a contributory factor [40].

2.4 Manufacture of Carbon Fibers

Since the early work of Edison, many types of precursors have been used to produce carbon fibers, of which polyacrylonitrile (PAN) has proved to be the most popular. The ideal requirements for a precursor are that it should be easily converted to carbon fiber, give a high carbon yield and allow to be processed economically. The attraction of PAN is that the polymer has a continuous carbon backbone and the nitrile groups are ideally placed for cyclization reaction to occur, producing a ladder polymer, believed to be the first stage towards the carbon structure of the final fiber. The carbon content of acrylonitrile (CH_2=CHCN) is 67.9% and it is not surprising PAN precursors have a carbon yield of some 50–55%, coupled with the ability to produce high modulus fibers. An acrylic fiber is defined as having acrylonitrile (AN) monomer content greater than 85%. Fibers with AN content less than 85% are termed modacrylics and are not suitable for use as carbon fiber precursors. A cellulosic precursor $(C_6H_{10}O_5)_n$ has a carbon content of 44.4% but, unfortunately, in practice, the reaction is more complicated than just simple dehydration and the carbon yield is only of the order of 25–30%. Pitch based carbon fibers, however, do have a higher yield of 85% with a high resultant modulus but, due to their more graphitic nature, they will have poorer compression and transverse properties as compared to PAN based carbon fibers. Other forms of precursor such as vinylidene chloride and phenolic resins have been investigated and have not been found to be commercially viable [54].

2.4.1 Pitch based Carbon Fibers

Pitch is a general name for the tarry substance, which is solid at room temperature and can be obtained from one of several sources:

1. Petroleum refining, normally called bitumen, or asphalt in the U.S.A.

2. Destructive distillation of coal

3. Natural asphalt, e.g. from Trinidad

4. Pyrolysis of PVC

5. Pyrolysis of ring compounds, such as naphthalene and anthracene

Pitch is a complex mixture of many hundreds of aromatic hydrocarbons, comprising structures with some three- to eight-membered rings, with alkyl side groups, normally methyl, with an average molecular weight of 300–400 [54].

The pitch based carbon fiber was developed by Otani and co-workers in 1963 and now it is recognized as an important industrial material. The pitches used as starting materials for the preparation of carbon fibers are by-products of the coke-making and petrochemical industries. For this reason, these materials have the advantage of being cheap precursors of carbon fibers. Pitch can be defined as a solid, fusible product of the pyrolysis of organic materials [60].

Natural pitch is a high molecular weight by-production of the destructive distillation of petroleum, coal, or natural asphalt. Pitches are composed of a wide variety of different generic classes of compounds ranging from low molecular weight paraffinic material at one extreme to very highly aromatic species at the other. In most types of pitches polycyclic aromatic hydrocarbons (PAH) comprise the dominant class of compounds. Partially hydrogenerated PAH occur in petroleum pitches in larger amounts but in high temperature coal-tar pitch the concentrations are low [65].

Pitch can be considered to be composed of four general classes of chemical compounds: Saturates, naphthene aromatics, polar aromatics, and asphaltenes. Saturates are the fraction of the pitch which consist of low molecular weight aliphatic compounds. Low molecular weight aromatics and saturated ring structures make up the naphthene aromatic portion of pitch. Polar aromatics, on the other hand, have a higher molecular weight and tent to be more heterocyclic in nature. Asphaltene is the highest molecular weight fraction in a pitch, and it also has the highest degree of aromaticity. Because it tends to consist of large, alkylated, plate-like molecules of condensed aromatic rings, the asphaltene fraction is the most thermally stable portion of the pitch [66].

The thermal stability, softening point, and potential carbon yield of a given pitch depend on the relative proportions of the four classes of chemical compounds that it contains. As one would expect, as the asphaltene fraction of a pitch increases, the

thermal stability and softening point tend to increase. In addition to increasing the thermal stability and softening of the pitch, a high apshaltene content often results in a high carbon yield when the pitch is converted to fiber. Coal tar pitches are, in general, more aromatic than petroleum pitches. The coal tar pitch has higher benzene and quinoline insoluble content but a lower average molecular weight. Since it is more aromatic and contains a higher benzene and quinoline insoluble content, one might expect coal tar pitch to have a high carbon yield, making it an obvious choice as a precursor for carbon fibers. And also coal tar pitch as a feedstock for the production of carbon fibers provides a relatively cheap raw material available in sufficient quantities, with the prospect of a high carbon yield [67].

Carbon fibers based on petroleum pitch have a unique property profile, which includes: very high axial modulus, strongly negative values of axial thermal expansion coefficient; high axial thermal and electrical conductivity, and adequate tensile properties [66].

Pitch based carbon fibers having a board range of microstructure and mechanical properties are available commercially. The fibers have high potential to be used as reinforcement in carbon/ carbon composites.

Pitch based carbon fibers have been recognized as a strategic material for the near future because of their excellent tensile properties. Tensile properties, such as Young's modulus and tensile strength of carbon fibers, strongly depend on the degree of preferred orientation in the graphitic layers along the fiber axis.

2.4.2 Rayon based Carbon Fibers

Figure **2.1**, shows the basic elements required for producing carbon filaments from rayon [68]. The first low-temperature treatment takes place typically at around 300 °C and converts the structure to a form which is stable to higher processing temperatures. The process involves polymerization and the formation of cross-links.

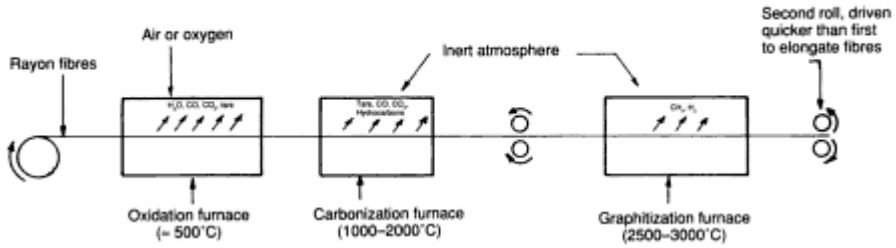

Figure 2.1: Basic elements required to produce carbon fibers from rayon.

The rayon may be subjected to a chemical treatment before the first-stage oxidation exposure. The chemical bath can be an aqueous ammonium chloride solution or a dilute solution of phosphoric acid in denatured ethanol. The chemical treatment serves to reduce the time for the low-temperature step from several hours to around 5 minutes. Of the fiber mass, 50-60% is lost to decomposition products such as H_2O, CO and CO_2 during oxidation. The carbonization step, resulting in further weight loss, is usually carried out at ≈1500 °C. The yield after carbonization is typically 20-25% of the original polymer weight. At this stage the fibers have an essentially isentropic structure. The mechanical properties of carbonized rayon are poor as a direct result of the poor alignment of the grapheme layers. Stretching of the fibers during heat treatment to graphitization temperatures significantly increases both strength and modulus, but is an expensive process. The morphology of the ex-rayon carbon fibers exhibits a crenulated surface, rather like a stick of celery, which is derived from the original precursor. The combination of poor mechanical properties, low carbon yield and expense of graphitization has meant that ex-rayon carbon fibers have generally not proved competitive in the market place, although they are used extensively in ablative technology. This is due to their poor through thickness thermal conductivity and because their composites yield high inter laminar shear strengths [69].

2.4.3 Vapor Grown Carbon Fibers

Primitive technology had being used for the preparation of vapour grown fibers as the 1889 patent of Hughes and Chambers, which describes the growth of ‘hair-like carbon filaments’, utilized a feedstock of hydrogen and metane pyrolysed in an iron crucible. The fibres were thought to be suitable for electric light bulb filaments, but lack of modern process controls made them uncompetitive [70].

Vapour grown carbon fibers are a promising new technology for the production of strong, stiff, discontinuous carbon fibers, which will be useful in applications where cost is an important consideration.

The basic process for producing vapour grown carbon fibers was developed by Gary Tibbetts. In this process, an organometallic compound containing iron is injected into a hydrocarbon vapour at temperatures above 1000 °C. The fibres were lengthen and thicken as they move through the reactor with the gas stream and collected as they exist. However, the process was non-productive; the iron catalyst did not grow filaments profusely enough to be a practical continuous reactor [70].

One of the most important problems in the growth of carbon fibers from catalyst particles is the role of sulphur in the process. As early as 1954, Kauffman and Griffiths were able to increase the fibre fraction of the product grown on silica reactor tube walls tenfold by adding 0.4% by volume H_2S to coke oven gas. During this epoch there was no recognition of the fact that the fibres were growing from small iron particles inadvertently present in the reactor. On the contrary, Katsuki et.al. showed that while iron was indeed a catalyst material, hydrogen sulphide, or sulphur in general, could have an even more crucial role [71]. This group showed more recently that sulphur addition to the iron catalyst particles alone made fibre growth much more profuse. More recently, Tibbets, et.al observed that 1% addition of hydrogen sulphide to the feedstock of continuous reactor, where abundant fibre nucleation is especially important, is vital to obtaining high yield fibre growth [70].

2.4.4 PAN based Carbon Fibers

In the production of PAN carbon fibers the PAN monomer is co-polymerized with 5-8 wt. % of another monomer such as acrylic acid, methylacrylate or vinyl acetate. These additions lower the glass transition temperature of the polymer and assist in the stabilization of the polymer during oxidation. PAN fibers are extruded into a filament form using solution spinning techniques.Figure 2.2 is a schematic diagram showing the details of this spinning process. In the solution spinning process the copolymer is first dissolved in a solvent such a diethylacetamide. The solution (15-30 wt. % polymer by weight) is extruded through a spinneret containing a large number of small (approximately 100 μm) holes. The solution then exits the spinneret and enters a coagulating bath, such as ethylene glycol, which extracts the solvent from polymer.

The use of solvents is costly and since the presence of solvents influences the final properties of carbon fibers, this approach has its limitations [72].

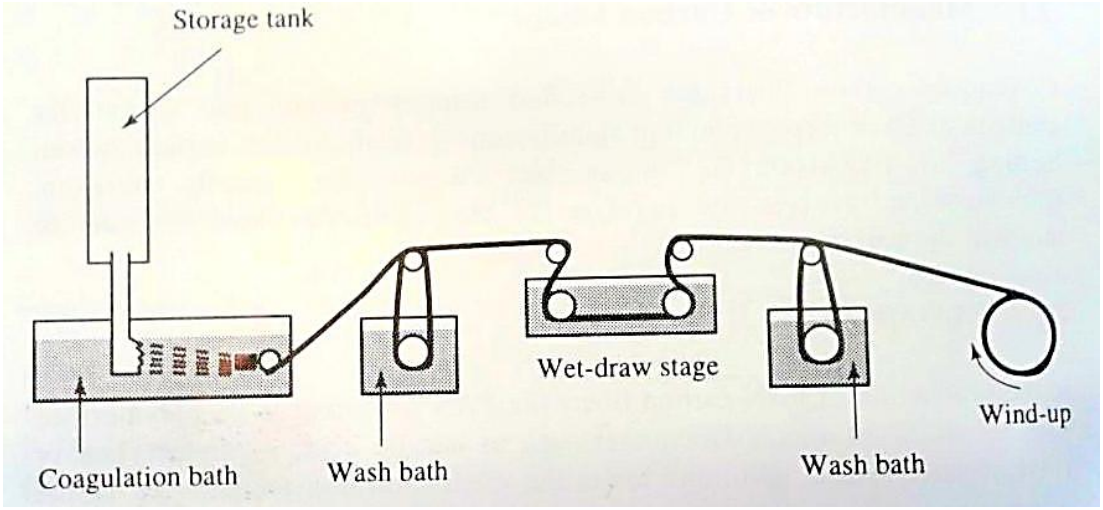

Figure 2.2: Schematic of the wet-spinning process of PAN/fibers.

Because of these limitations BASF Inc. developed a melt-assisted process to produce PAN based carbon fibers. In this melt-assisted process the copolymer is purified and dewatered before extrusion. Following polymerization, the PAN copolymer is extruded through a spinneret directly into a steam-pressurized solidification zone. The fibers are then stretched and dried. This melt assisted spinning process eliminates the need for expensive solvents and results in a uniform fiber structure.

PAN fibers are stabilized in order to retain their shape and structure during carbonization. The stabilization of PAN fibers is conducted in an oxidizing environment at 200-300 ºC under tension. Stabilization converts the thermoplastic PAN fibers into a non-plastic compound that is capable of withstanding carbonization hear treatment temperatures (1000-1600 ºC). In addition, the oxidation of the PAN fibers is required to develop the aromatic structure. During the oxidation of PAN, numbers of chemical reactions occur including the cyclization of the nitrile groups, and dehydrogenation of the saturated carbon-carbon bonds which facilitate the development of the aromatic structure in the fiber [31].

The oxidation of PAN fibers is performed in a large box-furnaces, in which the fibers are processed under a controlled tension. Tension is required in order to prevent the oriented structure of the polymer, obtained during the spinning process, from relaxing.

Following stabilization, the PAN fibers are carbonized and occasionally graphitized in an inert atmosphere to temperatures between 1000 and 2800 ºC.

The homopolymer PAN is not an easy product to process into carbon fiber, since the initial oxidation stage of the carbon fiber process is a difficult reaction to control due to the sudden and rapid evolution of heat, coupled with a relatively high initiation temperature.

This rapid surge of heat can cause chain scission with resultant poor carbon fiber properties. As far as is known, homopolymer PAN has never been exploited as a precursor for carbon fiber manufacture. The exothermic reaction can, however, be adequately controlled by suitable comonomers such as itaconic acid.

3. ELECTRO SPINNING

Electrospinning, a broadly used technology for electrostatic fiber formation which utilizes electrical forces to produce polymer fibers with diameters ranging from 2 nm to several micrometers using polymer solutions of both natural and synthetic polymers has seen a tremendous increase in research and commercial attention over the past decade[73–76]. This process offers unique capabilities for producing novel natural nanofibers and fabrics with controllable pore structure [77, 78].

Electrospinning is an old technique. In 1897 by Rayleigh observed for first time and studied in detail by Zeleny[79] on electrospraying. The work of Taylor[80] on electrically driven jets has laid the groundwork for electrospinning. The term "electrospinning", derived from "electrostatic spinning". From 1934 to 1944, Formhals published a series of patents, describing an experimental setup for the production of polymer filaments using an electrostatic force [81].

Electrospinning is one of the spinning techniques with a unique approach using electrostatic forces to produce fine fibers from polymer solutions or melts and the fibers thus produced have a thinner diameter (from nanometer to micrometer) and a larger surface area than those obtained from conventional spinning processes. Furthermore, a DC voltage in the range of several tens of KVs is necessary to generate the electrospinning. Various techniques such as electrostatic precipitators and pesticide sprayers work similarly to the electrospinning process and this process, mainly based on the principle that strong mutual electrical repulsive forces overcome weaker forces of surface tension in the charged polymer liquid [82]. Currently, there are two standard electrospinning setups, vertical and horizontal. With the expansion of this technology, several research groups have developed more sophisticated systems that can fabricate more complex nanofibrous structures in a more controlled and efficient manner [83]. Electrospinning is conducted at room temperature with atmosphere conditions.

The schematic set up of electrospinning apparatus which was used in this work shown in Figure **3.1**. Basically, an electrospinning system consists of three major components: a high voltage power supply, a spinneret (e.g., a nozzle tip) and a grounded collecting plate (usually a metal screen, plate, or rotating mandrel) and utilizes a high voltage source to inject charge of a certain polarity into a polymer solution or melt, which is then accelerated towards a collector of opposite polarity [84, 85]. Most of the polymers are dissolved in some solvents before electrospinning, and when it completely dissolves, forms polymer solution [82].

Schematic illustration of Exerted force on the tip of the capillary also illustrated in the Figure 3.1.

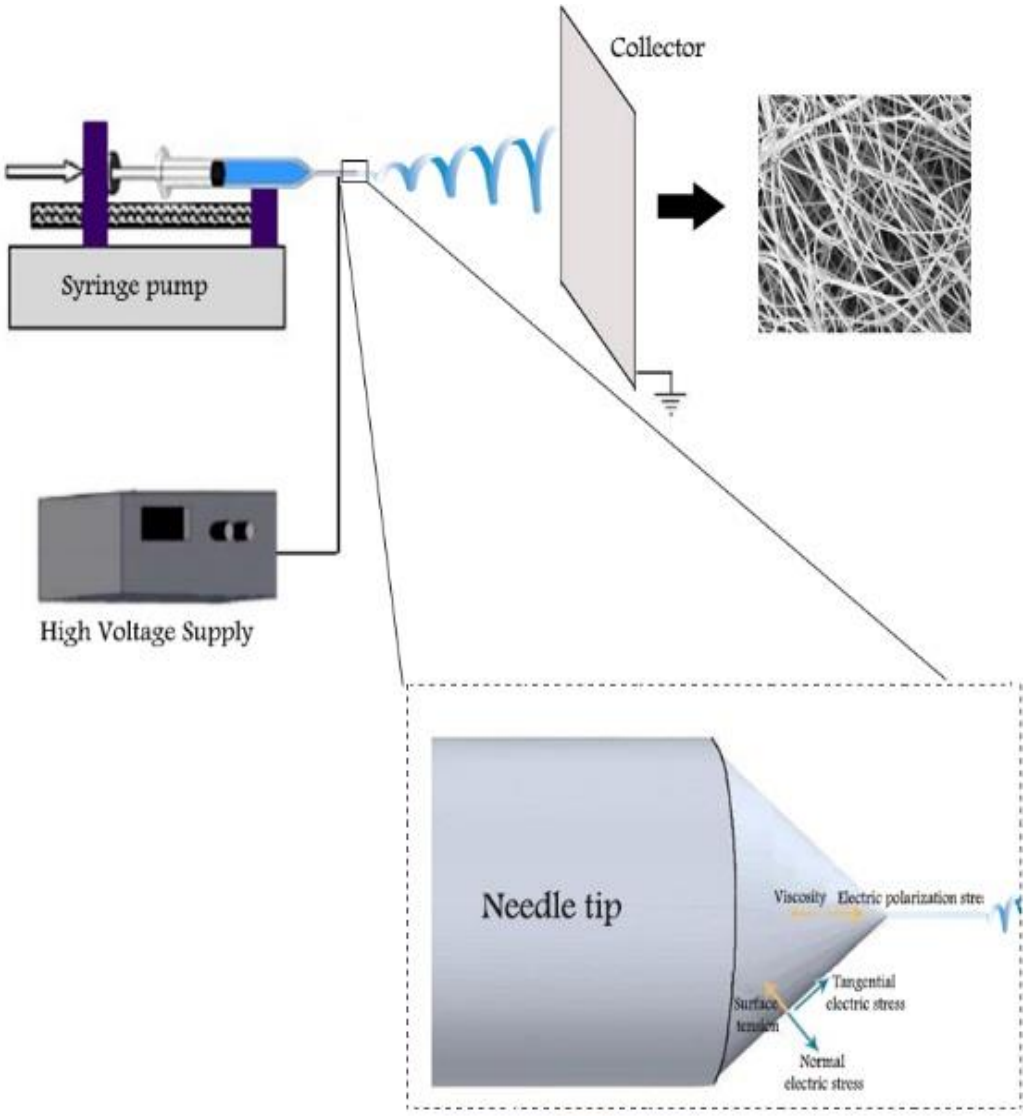

Figure 3.1: Schematic illustration of the experimental apparatus.

3.1 Polymers and copolymers used in electrospinning

There are a wide range of polymers that used in electrospinning and are able to form fine nanofibers within the submicron range and used for varied applications. Electrospun nanofibers have been reported as being from various synthetic polymers or natural polymers. Over the years, more than 200 polymers have been electrospun successfully from several natural polymers and characterized with respect to their applications.

Electrospinning with copolymers offers property enhancement of polymeric materials, including modifying of thermal stability, mechanical strength and barrier properties, and has therefore been often pursued for engineering structural applications.

The use of copolymers is a viable scheme to generate new materials of desirable properties and when properly implemented, the performance of electrospun scaffolds based on copolymers can be significantly improved as compared to homopolymers. Biodegradable hydrophobic polyesters generally have good mechanical properties but lack cell affinity for tissue engineering, but with the incorporation of a proper hydrophilic polymer segment, there is increase in the cell affinity. Apart from the cell affinity, the mechanical properties, morphology, structure, pore size and distribution, biodegradability and other physical properties can also be tailored by the use of copolymers in electrospinning.

Thus, copolymers based electrospinning appears as an attractive option for enhancing the properties of polymers for tissue engineering applications [3, 82].

3.2 Effects of various parameters on electrospinning

As mentioned above, the electrospinning process is solely governed by many parameters, classified broadly into solution parameters, process parameters, and ambient parameters. Solution parameters include viscosity, conductivity, molecular weight, and surface tension and process parameters include applied electric field, tip to collector distance and feeding or flow rate. Each of these parameters significantly affect the fibers morphology obtained as a result of electrospinning, and by proper manipulation of these parameters we can get nanofibers of desired morphology and diameters [86].

In addition to these variables, ambient parameters encompass the humidity and temperature of the surroundings which play a significant role in determining the morphology and diameter of electrospun nanofibers [87].

3.2.1 Solution parameters

Solution parameters in electrospinning method play crucial role in the final product nano-fibers. For instance they directly affected fibers diameters. Concentration, molcular weight, viscosity and surface tension of the sulotion are the main terms which studied in the literature and mentioned as below distinctly.

3.2.1.1 Concentration

In the electrospinning process, for fiber formation to occur, a minimum solution concentration is required. It has been found that at low solution concentration, a mixture of beads and fibers is obtained and as the solution concentration increases, the shape of the beads changes from spherical to spindle-like and finally uniform fibers with increased diameters are formed because of the higher viscosity resistance [88, 89]. There should be an optimum solution concentration for the electrospinning process, as at low concentrations beads are formed instead of fibers and at high concentrations the formation of continuous fibers are prohibited because of the inability to maintain the flow of the solution at the tip of the needle resulting in the formation of larger fibers [90]. Researchers have attempted to find a relationship between solution concentration and fiber diameter and they found a power law relationship, that increasing the concentration of solution, increases the fiber diameter with gelatin electrospinning [89, 91].

3.2.1.2 Molecular weight

In addition to solution concentration, molecular weight of the polymer has a significant effect on rheological and electrical properties such as viscosity, surface tension, conductivity and dielectric strength [88]. This is the other important solution parameter that affects the morphology of electrospun fiber and generally high molecular weight polymer solutions have been used in electrospinning as they provide the desired viscosity for the fiber generation.

low a molecular weight solution tends to form beads rather than fibers and a high molecular weight solution gives fibers with larger average diameters. Molecular weight of the polymer reflects the number of entanglements of polymer chains in a solution, thus solution viscosity. Gupta et al. have synthesized PMMA varying in molecular weight from 12.47 to 365.7 kDa to investigate the effect of molecular weight of the polymer, and they found that as the molecular weight increased, the number of beads and droplets decreased [92]. It has been observed that high molecular weights are not always essential for the electrospinning process if sufficient intermolecular interactions can provide a substitute for the interchain connectivity obtained through chain.

3.2.1.3 Viscosity

The other solution parameter which plays an important role in determining the fiber size and morphology during spinning of polymeric fibers, is viscosity. It has been found that with very low viscosity there is no continuous fiber formation and with very high viscosity there is difficulty in the ejection of jets from polymer solution, thus there is a requirement of optimal viscosity for electrospinning. The viscosity range of a different polymer solution at which spinning is done is different. Researchers have reported maximum spinning viscosities ranging from 1 to 215 poise [93–95].

3.2.1.4 Surface tension

Surface tension, more likely to be a function of solvent compositions of the solution plays a critical role in the electrospinning process and by reducing the surface tension of a nanofiber solution, fibers can be obtained without beads. Different solvents may contribute different surface tensions. Generally, the high surface tension of a solution inhibits the electrospinning process because of instability of the jets and the generation of sprayed droplets[96]. The formation of droplets, bead and fibers depends on the surface tension of solution and a lower surface tension of the spinning solution helps electrospinning to occur at a lower electric field [88].

However, not necessarily a lower surface tension of a solvent will always be more suitable for electrospinning. Basically, surface tension determines the upper and lower boundaries of the electrospinning window if all other variables are held constant [97, 98].

3.2.2 Processing parameters

The effects of electrospinning processing parameters such as the voltages which applied on the tip of the nozzle, flow rate of polymer from syringe, different types of collectors and finally the distance between the tip of nozzle and collector on the structure of fibers studied before and summarize as below.

3.2.2.1 Applied voltage

In the electrospinning process a crucial element is the applied voltage to the solution. Only after attainment of threshold voltage, fiber formation occurs, this induces the necessary charges on the solution along with electric field and initiates the electrospinning process. It has been already proved experimentally that the shape of the initiating drop changes with spinning conditions (voltage, viscosity, and feed rate). There is a little dispute about the behaviour of applied voltage in the electrospinning process [99]. have showed that there is not much effect of electric field on the fiber diameter with electrospinning of polyethylene oxide. Researchers have suggested that when higher voltages are applied, there is more polymer ejection and this helps the formation of a larger diameter fiber [97, 100]. Other authors have reported that an increase in the applied voltage (i.e., by increasing the electric field strength), increases the electrostatic repulsive force on the fluid jet which ultimately favours the narrowing of fiber diameter. In most cases, a higher voltage causes greater stretching of the solution due to the greater columbic forces in the jet as well as a stronger electric field and these effects lead to reduction in the fiber diameter and also rapid evaporation of solvent from the fibers results. At a higher voltage there is also greater probability of beads formation [88, 94, 101]. Thus, voltage influences fiber diameter, but the level of significance varies with the polymer solution concentration and on the distance between the tip and the collector [102].

3.2.2.2 Feed rate/Flow rate

The flow rate of the polymer from the syringe is an important process parameter as it influences the jet velocity and the material transfer rate. A lower feed rate is more desirable as the solvent will get enough time for evaporation. There should always be a minimum flow rate of the spinning solution. It has been observed that the fiber diameter and the pore diameter increases with an increase in the polymer flow rate in the case of polystyrene (PS) fibers and by changing the flow rate, the morphological

structure can be slightly changed. High flow rates result in beaded fibers due to unavailability of proper drying time prior to reaching the collector [103, 104].

3.2.2.3 Types of collectors

The another important aspect of the electrospinning process is the type of collector used. In this process, a collector serves as a conductive substrate where the nanofibers are collected. Generally, aluminium foil is used as a collector but due to difficulty in transferring of collected fibers and with the need for aligned fibers for various applications, other collectors such as, conductive paper, conductive cloth, wire mesh, pin, parallel or grided bar, rotating rod, rotating wheel, liquid non solvent such as methanol coagulation bath and others are also commontypes of collectors nowadays [82].

In the blowing-assisted electrospinning of hyaluronic acid, Wang et al. used two kinds of collector aluminium foil and wire screen and found that a less conductive area of wire screen imposes a negative effect on fiber collection. With less conductive area, there was generation of beaded fibers because of the less surface area[105]. In another study they compared wire screen with aluminium foil and wire screen without aluminium foil in the same conductive area and found that pure wire screen is a better collector for fiber collection because with the use of wire screen the transfer of fibers to other substrates became easy. The fiber alignment is determined by the type of the target/collector and its rotation speed. The generated nanofibers are deposited on the collector as a random mass due to the bending instability of the highly charged jet. Several research groups have demonstrated the use of a rotating drum or a rotating wheel-like bobbin or metal frame as the collector, for getting aligned electrospun fibers more or less parallel to each other [94].

3.2.2.4 Tip to collector distance

The distance between the tip and the collector has been examined as another approach to control the fiber diameters and morphology. It has been found that a minimum distance is required to give the fibers sufficient time to dry before reaching the collector, otherwise with distances that are either too close or too far, beads have been observed [89]. The effect of tip and the collector distance on fiber morphology is not as significant as other parameters and this has been observed with electrospinning of PVA [97]. It has been reported that flatter fibers can be produced at closer distances

but with increase in distance rounder fibers have been observed with the spinning of silk-like polymer with fibronectin functionality [95]. One important physical aspect of the electrospinning nanofibers is their dryness from the solvent used to dissolve the polymer [106]. Thus, there should be optimum distance between the tip and collector which favours the evaporation of solvent from the nanofibers.

3.2.3 Ambient parameters

There are also ambient parameters that include humidity, temperature etc which is effective on the structure of the electrospun fibers. Studies have been conducted to examine the effects of ambient parameters (i.e., temperature and humidity) on the electrospinning process. Mit- Uppatham et al. have investigated the effect of temperature on the electrospinning of polyamide-6 fibers ranging from 25 to 60 °C and found that with increase in temperature, there is a yield of fibers with decreased fiber diameter. In order to the fact that there is an inverse relationship between viscosity and temperature, they attributed the fiber decline in diameter to the decrease in the viscosity of the polymer solutions at increased temperatures[107].

The variation in humidity while spinning polystyrene solutions has been studied and shows that by increasing humidity there is an appearance of small circular pores on the surface of the fibers; further increasing the humidity leads to the pores coalescing [108]. It has been found that at very low humidity, a volatile solvent may dry rapidly as the evaporation of the solvent is faster. Sometimes the evaporation rate is so fast than compared to the removal of the solvent from the tip of the needle and this would create a problem with electrospinning. As a result, the electrospinning process may only be carried out for a few minutes before the needle tip is clogged [93]. Hence, apart from solution and processing parameters, ambient parameters also affect the electrospinning process.

3.3 Solvents used for electrospinning

The solvent used in preparing polymer solutions has a significant influence on its spinnability, because the first and foremost step in the electrospinning process is dissolution of polymer in a suitable solvent. Solvents should have some properties such as, good volatility, vapour pressure, boiling point and should maintain the integrity of

the polymer solution. Thus for successful electrospinning the selection of an appropriate solvent system is indispensable.

As stated above, in electrospinning, rapid solvent evaporation and phase separation occurs due to jet thinning, solvent vapour pressure plays a critical role in determining the evaporation rate and the drying time. Solvent volatility also plays a significant role in the formation of nanostructures as it influences the phase separation process. It is well known that the morphology and size of electrospun nanofibers strongly depend on solution properties such as, viscosity and surface tension. Different solvents may contribute different surface tensions.

The solution viscosity is determined by the concentration of the polymer, but the value of surface tension depends on both the polymer and solvent [99].

It has been recognized that surface tension seems more likely to be a function of solvent compositions, but is negligibly dependent on the polymer concentration. A lower surface tension of the solvent is not always necessarily suitable for electrospinning [109].

The properties of solvents have a profound effect on fiber diameter. Basically, a solvent performs two crucial roles in electrospinning: firstly to dissolve the polymer molecules for forming the electrified jet and secondly to carry the dissolved polymer molecules towards the collector [110].

The solvents used in electrospinning of polymers can provide very useful information for understanding the effects of solution properties such as conductivity. Dimethylformamide (DMF), a dipolar aprotic solvent, which has a high dielectric constant and dipole moment, has been successfully used as a solvent for electrospinning of poly (acrylonitrile) and poly(acrylonitrile-co-vinyl acetate) and poly(acrylonitrile-co-itaconic acid) copolymers electrospinning and its addition enhances the solution conductivity which is a prerequisite for the formation of bead free uniform fibers[3, 5, 111].

The effect of varying concentrations of solvents, acetic acid has been observed for chitosan electrospinning, and it was found that by increasing the concentration of solvent, there was a gradual decrease in surface tension of the solution which favoured production of thinner fibers [82].

For summarizing all mentioned above, important features of electrospinning listed as below:

- Suitable solvent should be available for dissolving the polymer.
- The vapor pressure of the solvent should be suitable so that it evaporates quickly enough for the fiber to maintain its integrity when it reaches the target but not too quickly to allow the fiber to harden before it reaches the nanometer range.
- The viscosity and surface tension of the solvent must neither be too large to prevent the jet from forming nor be too small to allow the polymer solution to drain freely from the pipette.
- The power supply should be adequate to overcome the viscosity and surface tension of the polymer solution to form and sustain the jet from the pipette.

The gap between the pipette and grounded surface should not be too small to create sparks between the electrodes but should be large enough for the solvent to evaporate in time for the fibers to form [112].

4. ACTIVATION OF CARBON NANO-FIBERS

Activated carbon, also called activated charcoal, activated coal, or carbo activatus, is a form of carbon processed to be riddled with small, low-volume pores that increase the surface area available for adsorption or chemical reactions. Activated is sometimes substituted with active.

Due to its high degree of microporosity, just one gram of activated carbon could has a surface area in excess of 200 m^2, as determined by adsorption isotherms of carbon dioxide gas at room or 0 °C temperature. An activation level sufficient for useful application may be attained solely from high surface area; however, further chemical treatment often enhances adsorption properties [1].

Basically, carbons are described as graphitic or non-graphitic depending upon degree of crystallographic ordering. Graphitic carbons possess three-dimensional symmetry while nongraphitic carbons do not. As discussed above, during carbonisation the free interstices present in the carbon become filled or at least partially blocked by disorganised “amorphous” carbon apparently as a result of deposition of tarry substances. The resulting carbonised product has only a very small adsorption capacity. Presumably, at least for carbonisation at lower temperature, part of the tar remains in the pores between the crystallites and on their surfaces. Such carbonised materials can be then at least partially activated by removing tarry products by heating in steam or under inert gas or by extraction with a suitable solvent or by chemical reaction.

Thus activation is carried out to enlarge the diameters of the pores which are created during the carbonisation process and to create some new porosity thus resulting in the formation of a well-developed and readily accessible pore structure with very large internal surface area.

Activation is carried out by two ways as in the following sections.

4.1 Production of Activated Carbon Fiber

Activated carbon is carbon produced from carbonaceous source materials such as nutshells, coconut husk, peat, wood, coir, lignite, coal, PAN and petroleum pitch. It can be produced by one of the following processes:[113]

4.1.1 Physical Reactivation

It is a process by which the carbonised product develops porous structure of molecular dimensions and extended surface area on heat treatment in the temperature range of 700–1000 ˚C in presence of suitable oxidising gases such as steam, CO_2, air (ACS 1996). Gasification of the carbonised material with steam and carbon dioxide occurs by the following endothermic reactions:

$C + H_2O \rightarrow CO + H_2$ (29 kcal),

$C + CO_2 \rightarrow 2CO$ (39 kcal),

$CO + H_2O \rightarrow CO_2 + H_2$ (10 kcal).

The H_2O molecule is smaller than the CO_2 molecule and diffuses faster into the pores of the carbon. Consequently reaction with steam is faster than that with CO_2.

Activation with CO_2 promotes external oxidation and development of larger pores as compared to activation with steam. The relative amounts of external and internal oxidation depends on how well-developed the pores are in the carbonised material.

Activation is associated with carbon loss and hence with decrease in weight of host carbon. Weight loss increases linearly with activation temperature and time. Activation at lower temperature predominate in the development of mesopores and macropores. Formation efficiency of pores which have no adsorption ability, i.e. macropores, increase at higher activation

temperature, while mean pore diameter decreases with increasing activation temperature.

In case of activation with oxygen, both the reactions

$C + O_2 \rightarrow CO_2 + 92.4$ kcal,

and

$2C + O_2 \rightarrow 2CO + 53.96$ kcal,

take place. Since both reactions are exothermic, there is excessive burning and the reaction is difficult to control. Moreover, since there is always some local overheating, the product obtained is not uniform.

As the reaction is very aggressive, burning is not restricted and also occurs on the surface of the fibers, causing excessive weight loss.

The source material is developed into activated carbons using hot gases. This is generally done by using one or a combination of the following processes:

- Carbonization: Material with carbon content is pyrolyzed at temperatures in the range 600–900 °C, in absence of oxygen (usually in inert atmosphere with gases like argon or nitrogen).
- Activation/Oxidation: Raw material or carbonized material is exposed to oxidizing atmospheres (carbon dioxide, oxygen, or steam) at temperatures above 250 °C, usually in the temperature range of 600–1200 °C.

4.1.2 Chemical Activation

Prior to carbonization, the raw material is impregnated with certain chemicals. The chemical is typically an acid, strong base, or a salt (phosphoric acid,potassium hydroxide, sodium hydroxide, calcium chloride, and zinc chloride 25%). Then, the raw material is carbonized at lower temperatures (450–900 °C). It is believed that the carbonization / activation step proceeds simultaneously with the chemical activation. Chemical activation is preferred over physical activation owing to the lower temperatures and shorter time needed for activating material.

Important production materials include coconut shells, palm shells, oil, husks, and sawdust, all of which have to be burnt into ashes for activated carbon making. It consists of two types; fine powder and pills or flakes. The fine powder is good at diffusing in water, so it is used in solution or liquid related industries. For example, it is used to bleach and absorb odor in sugar industry, to produce cooking oil in food industry, and to purify water. The pill or flake type is used in gas-purifying industries and products; such as, air purifier, poisonous gas absorbtion, and cigarette butt, etc.

The growth of activated carbon market depends on the growth of industries that use it, which vary greatly from air purifier industry, drinking water and tap water industry, metal-plated industry, and food industry. In addition, activated carbon can be used in

a household. Its major household usage is found in products that absorb odors; such as a refrigerator's stuffy smell, wardrobe's and closet's smells, etc. Hence, it can be seen that activated carbon market is broad and has a potential for consistent demand in the country. Besides, it can be exported to use in the industries that need high quality activated carbon; such as, in particular kinds of air purifiers. However, the import figures are still higher than the export [114].

In other words the structure of the pores and pore size distribution are largely dictated by the nature of the raw materials and the history of their carbonisation. Carbon atoms differ from each other in their reactivity depending on their spatial arrangement. Activation eliminates the disorganised carbon, exposing the aromatic sheets to the action of activation agents and leads to development of a microporous structure. Since activation is associated with weight loss of the host carbon, the extent of burn-off of the carbon material is taken as a measure of the degree of activation [115].

At a particular temperature, weight loss increases linearly with activation time. Normally, in the first phase, the deorganised carbon is burnt preferentially when the burn-off is about 10%. This results in the opening of blocked pores. Subsequently, the carbon of the aromatic ring system starts burning, producing active sites and wider pores.

In the latter phase, excessive activation reaction results in knocking down of the walls by the activated agents and a weight loss of more than 70%. This results in an increase in transitional pores and macropores. The volume of the micropores decreases and there is no significant increase in adsorption capacity or internal surface area.

At higher burn-off, the difference in porosity created by different activating agents become more pronounced. In a typical example, activation of a hard wood with water vapour results in progressive development and widening of all size pores until, at a burn-off of 70%, the activated product contains a well-developed porous system with wide pore size distribution. Activation with 50–70% burn-off causes an increase in the total adsorption volume from 0.6 to 0.83 cm^3/gm. But as it is associated mainly with widening of pores, the surface area remains almost the same. Activation with carbon dioxide mainly develops microporosity over the entire range of burn-off. The micropores account for about 73% of the total adsorption pore volume, for over 90% of total surface area. The micropores contribute only 33% towards total pore volume

and 63% towards surface area in the case of steam-activated carbon. Thus carbon produced by CO_2 activation has lower total pore volume (0.49 cm^3/gm) than those of corresponding samples obtained by activation of steam. However the effective surface area in both cases is almost the same. This is mainly due to the contribution of micropores to the surface area [116].

Furthermore, the carbon atoms which are localised at the edges and the margin of the aromatic sheets or those located at defect position and dislocations or discontinuities are associated with unpaired electron or have residual valancies, these are rich in potential energy. Consequently, these carbon atoms are more reactive and have a tendency to form surface oxygen complexes during oxidative activation [116].

These surface chemical groups promote adsorption and are beneficial in certain applications. Alternatively, these surface oxygen complexes break down and peel off the oxidised carbon from the surfaces as gaseous oxides leaving behind new unsaturated carbon atoms for further reaction with an activating agent.

Thus, activation mechanism can be visualised as an interaction between the activating agent and the carbon atoms which form the structure of intermediate carbonised product resulting in useful large internal surface area with interconnected pores of desired dimension and surface chemical groups.

Carbonisation of synthetic precursors such as phenolic, polyfurfuryl alcohol, polyacrylonitrile, saran etc. result in glass-like carbons with closed porosity. Activation of these chars, therefore, requires very stringent conditions of temperature, time and environment.

Summarizing the recent topic lead to the following paragraphs:

the In general, two main methods for the preparation of activated carbons are used: physical and chemical activation methods. Physical activation consists of a two-step process carried out at high temperature (700°C-1000°C), that is, carbonization under inert gas,normally nitrogen, and activation under oxidizing agents, as a rule, carbon dioxide or water vapor. On the other hand, chemical activation requires the treatment of the initial material with a dehydrating means.

for example, sulfuric acid, phosphoric acid, zinc chloride, potassium hydroxide, or others, at temperatures varying from 400°C to 1000°C, followed by the elimination of the dehydrating agent by meticulous washing.

A flow chart of the physical activation method is shown in Figure 4.1-(a). The standard chemical activation procedure is similar to the physical method of activation. That is, the dried raw material is crushed and sieved to the desired size fraction. Afterward, the obtained powdered material is mixed with a concentrated solution of a dehydrating compound. subsequently, this blend is dried and heated under inert atmosphere in furnace up to 400˚C-700˚C, and held at this temperature fot several hours; finally, the resulting material is thoroughly washed, dried, and conditioned.

In Figure 4.1-(b) a flow chart of chemical activation method is shown [117].

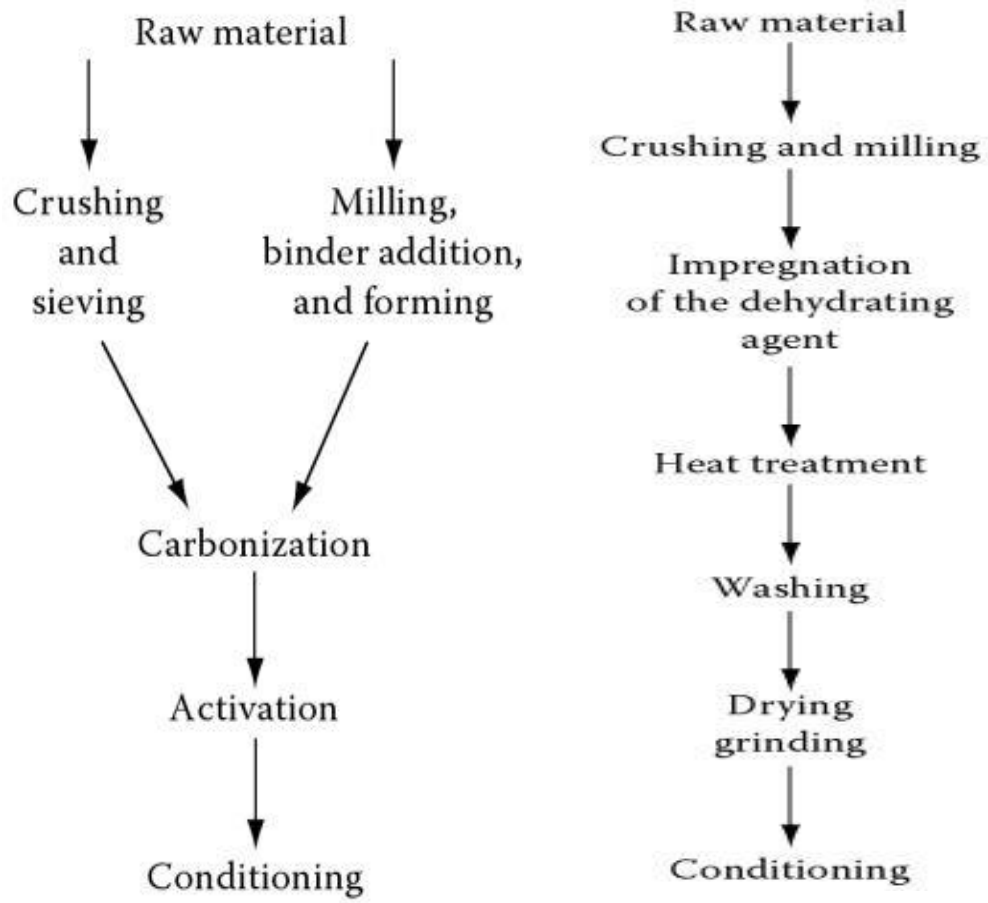

(a) (b)

Figure 4.1: flow chart of (a): The physical activation method, (b): The chemical activation method.

4.2 Properties of Activated Carbon Fiber and ACNFs

A gram of activated carbon can have a surface area in excess of 500 m^2, with 1500 m^2 being readily achievable. Carbon aerogels, while more expensive, have even higher surface areas, and are used in special applications [55].

Under an electron microscope, the high surface-area structures of activated carbon are revealed. Individual particles are intensely convoluted and display various kinds of porosity; there may be many areas where flat surfaces of graphite-like material run parallel to each other, separated by only a few nanometers or so. Tests of adsorption behaviour are usually done with nitrogen gas at 77 K under high vacuum, but in everyday terms activated carbon is perfectly capable of producing the equivalent, by adsorption from its environment, liquid water from steam at 100 °C and a pressure of 1/10,000 of an atmosphere.

Physically, activated carbon binds materials by Van der Waals force or London dispersion force.

Activated carbon does not bind well to certain chemicals, including alcohols, glycols, strong acids and bases, metals and most inorganics, such as lithium, sodium, iron, lead, arsenic, fluorine, and boric acid.

Activated carbon can be used as a substrate for the application of various chemicals to improve the adsorptive capacity for some inorganic (and problematic organic) compounds such as hydrogen sulfide (H_2S), ammonia (NH_3), formaldehyde (HCOH), radioisotopes iodine-131 and mercury (Hg). This property is known as chemisorptions [118].

4.3 Application of Activated Carbon Fibers and Nano-Fibers

Activated carbon is used in gas purification, decaffeination, gold purification, metal extraction, water purification, medicine, sewage treatment, air filters in gas masks and respirators, filters in compressed air and many other applications.

One major industrial application involves use of activated carbon in the metal finishing field. It is very widely employed for purification of electroplating solutions. For example, it is a main purification technique for removing organic impurities from bright nickel plating solutions. A variety of organic chemicals are added to plating

solutions for improving their deposit qualities and for enhancing properties like brightness, smoothness, ductility, etc. Due to passage of direct current and electrolytic reactions of anodic oxidation and cathodic reduction, organic additives generate unwanted break down products in solution. Their excessive build up can adversely affect the plating quality and physical properties of deposited metal. Activated carbon treatment removes such impurities and restores plating performance to the desired level [69].

5. EXPERIMENTAL

5.1 Materials

As mentioned before, CNFs was obtained in this study from various precursors. These precursors are AN homopolymers, P(AN-co-VAc) and P(AN-co-IA) copolymers.Acrylonitrile (99.5>%) and Vinylacetate (99.5 %) was provided by the AKSA Acrylic Chemistry Company. Itaconic acid (99.5>%) was obtained from Sigma Aldrich. Ammoniumpersulfate (APS), (99.5>%), dimethylformamide (DMF) and ethanol were provided from Sigma Aldrich.

The structural formulas of the precursors was given in Figure **5.1**.

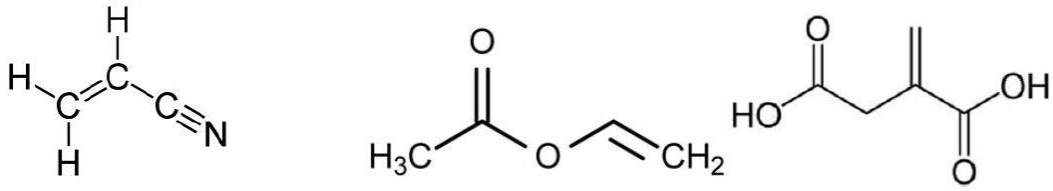

Acrylonitrile **Vinyl acetate** **Itaconic acid**

Figure 5.1: structural formula of Acrylonitrile, Vinyl acetate and Itaconic acid.

5.1.1 Synthesis of Precursors

Copolymerization of acrylonitrile/vinylacetate and acrylonitrile/itaconic acid comonomers were made by free radical polymerization. The polymerization technique is solution polymerization technique. APS was used as initiator. The polymerization is accesed in a three necked flask. The total monomer feed was 10 g for copolymers and homopolymer of PAN. The monomers were mixed in the three necked flask for 20 minutes. 0.8 g APS is dissolved in 30 ml of distilled water and added to the monomer mixture. The total mixture was 70 ml. The monomer feed ratios for copolymers were 85:15 (AN:VAc) and 85:15 (AN:IA). The polymerizations were

proceed at 60° C. The polymerization were completed generally in 3 hours. The synthesized polymer is washed with excess ethanol and distilled water. The filtered polymers are dried under the vacuum for 12 hours. The PAN homopolymer was synthesized by the same process. The APS amounts were same for all polymerization processes [111].

Table 5.1: Precursors which is used in this study.

Precursor	Name	% W
1	PAN	100
2	(AN:VAc)	(85:15)
3	(AN:IA)	(85:15)

5.2 Electrospinning

The polymer solution was held in horizontal syringe with a tip opening around 0.8 mm in diameter. A stainless steel electrode was immersed in the solution and connected to a high voltage power supply which could generate DC voltage up to 30 kV. A flat metal plate with aluminum foil placed across served as a vertical counter electrode. The voltage between the electrode and the counter electrode could be controlled by high voltage power supply. The air pressure behind the solution was controlled with an air pump so that a stable drop of the solution was suspended at the tip of the capillary before the power was supplied. The applied voltage between the tip and collector were set at 16 kV with a tip-to-collector distance of 16 cm and the flow rate of the feed is set as 1 ml/h. The fibers were collected on the aluminum foil in the form of nonwoven fabric [119].

5.3 Heat treatment

As stated in the previous sections, heat treatment of the carbon fibers precursors is the crucial factor to obtain appropriate carbon fiber. Stabilization, carbonization and activation are the main purpose of these steps of the heat treatment which has been applied to the precursors.

Thermal stabilization, carbonization and activation were carried out continuously in a horizontal tubular furnace (Carbolite 1 & 3 Zone Wire-Wound). The internal temperature of the furnace was first calibrated and then the length and position of the constant temperature hot zone determined. About 0.5–1 g of nanofibers were placed in a 10 cm quartz boat (open ends to facilitate gas flow) and positioned in the center of the constant temperature zone. Figure 5.2 illustrate the heat treatment set-up of this work.

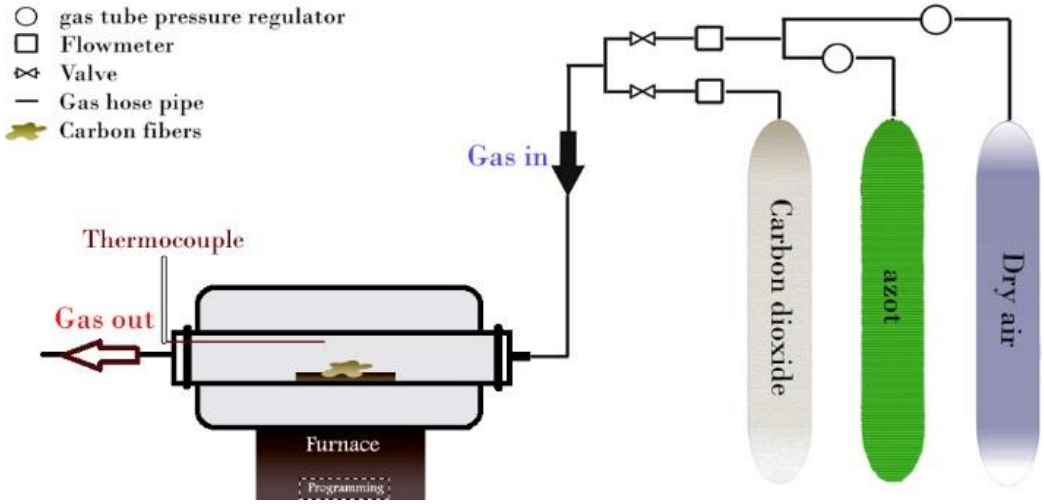

Figure 5.2: Schematic heat treatment set-up.

Thermal stabilization of the nanofibers was carried out by heating the samples to 230 °C at a rate of 1 °C.min^{-1} under a constant dry air flow of 0.5 L.min^{-1}. A soak time of 2 hours was applied at this temperature (230 °C).

Consecutive step namely carbonization was carried out by changing the feed gas from dry air to nitrogen with a flow of 1 L.min−1 and raising the temperature at a rate of 1 °C.min^{-1} to 300 °C.This was followed by changing the temperature ramp rate to 5 °C.min^{-1} up to 600 °C and maintaining the samples at this temperature for 60 min.

The carbonization was also followed by activation process. Activation was carried out by raising the temperature at a rate of 5 °C.min^{-1} to 750 °C. Having reached the specified temperature, CO_2 flow of 1 L.min^{-1} was switched on for 1 h.

Finally, just after CO_2 valve had closed and N_2 valve opened (1 L.min^{-1}) and samples were allowed to cool down (below 50 °C) before being removed from the furnace

taken out from the furnace. Figure **5.3** illustrate the heating regim which are used in consecutive steps of this study.

.

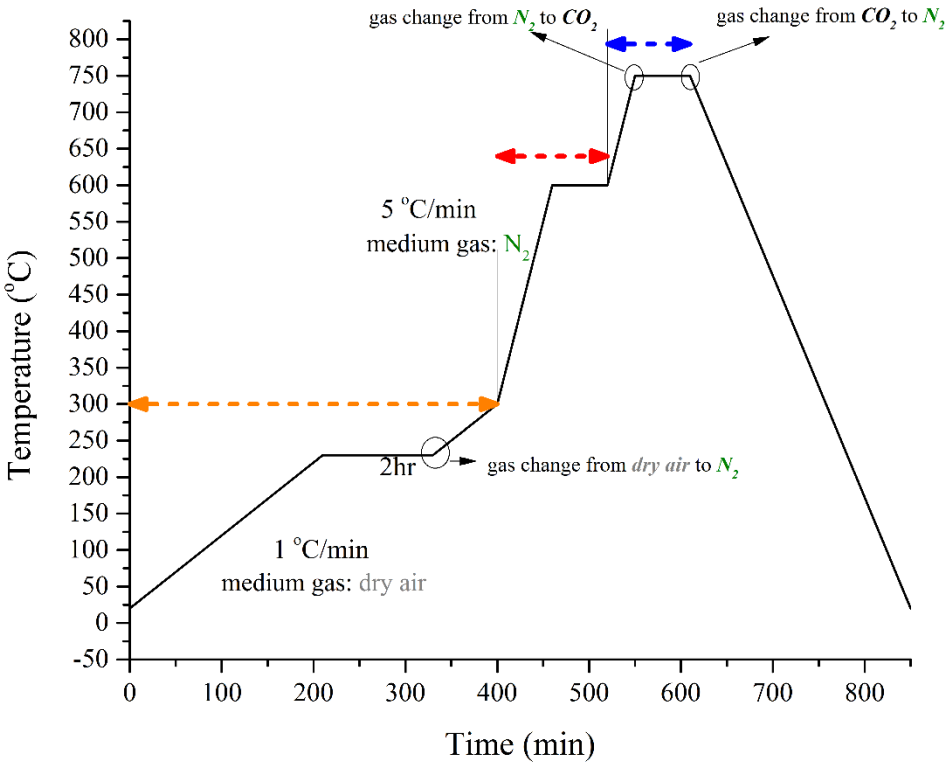

Figure 5.3: Heating regim illustration.

As shown in Figure **5.3** the orange, red and blue dash-arrows represented the oxidative stabilization, carbonization and activation region, respectively.

5.4 Characterization

The samples obtained were subjected to characterization at various steps of heat treatment. For this purpose, TGA, SEM, Porosity analysis and FTIR were used. In the following of this section concise and precise explanation about these characteriation methods prepared.

5.4.1 TGA

Thermal Gravimetric Analysis (TGA) has used to make quantitative measurements of any mass change caused by a transition or thermal degredation in the sample. TGA

measures the change in mass due to dehydration, decomposition, or oxidation of a polymer with time and temperature. Due to the unique sequence of the physicochemical reaction occuring at specific temperature range and heat rate and being a fuction of molecular structure, thermogravimetric curves are specific for a given polymer or compound. TGA curves, data concerning the thermodynamics and kinetics of the various chemical reactions, reaction mechanisms and the intermediate and final reaction products have obtained. Other processes that can be studied by TGA are adsorption and desorption phenomena, reactions with purge gases, ash content analysis, quantitative determination of additives, solid-state reaction composition of filled polymers, rates of evaporation, sublimation and at the estimation flame-retardancy of polymers [120].

The principle of thermogravimetric analysis is based on a thermobalance which describes an instrument continuously measures the weight changes of a substance at gradually varying temperatures [121].

In this study thermal gravimetric analysis is used to describe the thermal degradation and stability of the synthesized copolymers. It is aimed to observe the polymers stability at wide temperature range varying from 30°C to 1000°C. Diamond TG/DTA device (Perkin Elmer Ins.) is used to examine some thermal properties of the copolymer samples.

5.4.2 SEM

A scanning electron microscope (SEM) is a type of electron microscope that produces images of a sample by scanning it with a focused beam of electrons. The electrons interact with atoms in the sample, producing various signals that could detected and that contain information about the sample's surface topography and composition. The electron beam has generally scanned in a raster scanpattern, and the beam's position has combined with the detected signal to produce an image. SEM can achieve resolution better than 1 nanometer. Specimens can be observed in high vacuum, in low vacuum, and (in environmental SEM) in wet conditions.

Activated carbon fiber and nano carbon fiber is characterized for morphology by scanning electron microscope. For this operation, JSM-6390LV model scanning electron microscope (JEOL USA) is used.

The taken images was accurately processed to obtain the fibers diameter and also the study on the effect of the heat treatment on the geometrical stucture of the fibers in

each steps. This processing carried out by “Image-Pro Plus” software which is one of the best applicable image processing softwares.

5.4.3 FTIR

Infrared spectroscopy is a commonly used method to investigate of polymer structure and the analysis of functional groups. IR spectrometers have used to study samples in the gaseous, liquid, and solid state, depending on the types of accessories used. IR has been used to characterized polymer blends, dynamics, surfaces, and interfaces, as well as chromatographic effluents and degradation products. It is capable of qualitative identification of the structure of unknown materials as well as the quantitative measurement of the components in a complex mixture [120].

In this study, FTIR has used with the ATR accessories. It has used to investigate the structure of the synthesized homopolymer and copolymer. Quantitative measurements of the specific group of the polymer has indicated. Perkin Elmer, Spectrum One, with a Universal ATR attachment with a diamond and ZnSe crystal model FTIR-ATR is used at the studies.

5.4.4 BET

BET theory is a well-known rule for the physical adsorption of gas molecules on a solid surface, that basis for an important analysis technique for the measurement of the specific surface area of a material.

In 1938, Stephen Brunaucr, Paul Hugh Emmett, and Edward Teller published an article [122] about the BET theory for the first time; "BET" consists of the first initials of their family names.

The concept of the theory is an extension of the Langmuir theory, which is a theory for monolayer molecular adsorption, to multilayer adsorption with the following assumptions:

(a) gas molecules physically adsorb on a solid in layers infinitely;

(b) there is no interaction between each adsorption layer;

(c) the Langmuir theory could applied to each layer.

The specific area of electrospun fibers and activated form of them was analysed using a Micromeritics ASAP 2010 (Accelerated Surface Area and Porosimetry System)

which provides high quality surface area (BET) and porosity measurement on different types of solid materials based on the gas adsorption theory. This experiment done at 77°K. Before the experiments the samples were degassed under vaccum at 450°C for 24 hours and 100°C for 48hours respectively for activated mode and the electrospun fibers before applying any heating regim.

Surface area of samples was determined by using Brunaeur, Emmett and Teller (BET) method. Barret-Joyner-Halenda scheme used for determinde Adsorption CumulativePore Volume of pores of sample. Also The Horvath-Kawazoe (HK) model which is a widely used method for determining pore-size distribution in a microporous material from a single adsorption isotherm used to determinde Maximum Pore Volume and Median Pore Diameters of the samples. For determining Micropore Surface Area Dubinin-Astakhov method used as well.

6. RESULTS AND DISCUSSION

The characterization investigation of the samples by thermal gravimetric analysis accomplished for study the thermal stability of the samples by repot the amount of sample's weight loss till 1000˚C in Nitrogen medium at a heating rate of 10°Cmin^{-1}.

Also the fibers morphology and porosity structure of the activated carbon nano fibers scrutinized by scanning electro microscopy(SEM) and accelarated surface area and porosimetry system (ASAP). All of the fiber samples diameter and BET surface area of the electropun and activated fibers and also adsorption isotherm , pore diametere and pore volume of activated fibers carried out and disccused in this work.

Finally fourier transform infrared (FTIR) technique used to demonstrated the specific chemical trasformation during the activation process and also throughout the oxidative stabilization procedure.

All the fiber samples which named by specific code shown in **Table 6.1**.

Table 6.1: Sample codes.

Code	Sample Explanation
P0H0	Electrospun Acrylonitrile homopolymer
C2H0	Electrospun Poly(acrylonitrile-co- itaconic acid)(85:15)%Wt.
C4H0	Electrospun Poly(acrylonitrile-co-vinyl acetate)(85:15)%Wt.
P0S	Stabilized Acrylonitrile homopolymer
C2S	Stabilized Poly(acrylonitrile-co- itaconic acid)(85:15)%Wt.
C4S	Stabilized Poly(acrylonitrile-co-vinyl acetate)(85:15)%Wt.
P0Ca	Carbonized Acrylonitrile homopolymer
C2Ca	Carbonized Poly(acrylonitrile-co- itaconic acid)(85:15)%Wt.
C4Ca	Carbonized Poly(acrylonitrile-co-vinyl acetate)(85:15)%Wt.
P0Act	Activated Acrylonitrile homopolymer
C2Act	Activated Poly(acrylonitrile-co- itaconic acid)(85:15)%Wt.
C4Act	Activated Poly(acrylonitrile-co-vinyl acetate)(85:15)%Wt.

6.1 Thermal gravimetric analysis (TGA)

During the activation process, loss-weight behaviors of AN homopolymer and two copolymers would recorded. The weight loss was multistage reactions and taken place at different temperatures.

The lowest thermal properties of electrospun PAN, P(AN-co-IA) and P(AN-co-VAc) nanofibers are investigated using TGA characterizations. The TGA results of the different P(AN-co-VAc), P(AN-co-IA) and PAN in electrospun, stabilization and activation modes are shown comparatively in Figure 6.1, Figure 6.2 and Figure 6.3 respectively.

After completing cyclization reaction and interchain polymerization of nitrile groups, PAN fiber decomposes at 295 °C. The homopolymer of AN showed the main thermal decomposition at about the mentioned temperature (295 °C). However, for compolymers which contained VAc thermal decomposition temperature was about 315°C and this themperature for P(AN-co-IA) copolymer was about 305°C.

To investigate the behaviors, TGA scans of samples P0H0, C2H0, and C4H0 were performed in Nitrogen medium at a heating rate of 10°Cmin^{-1}, as shown in Figure 6.1.

The lowest initial loss-weight temperature was sample P0H0 (at 295°C), followed by C2H0 (305°C) and C4H0 (315°C). These values for copolymers higher than that of homopolymer of AN, indicating that thermal stability of PAN is improved after being copolymerized with VAc, and thus confirming the effect of VAc and IA functional groups existed in copolymers in addition to nitrile groups of PAN. These results are in good accordance with literature [5, 27].

Under initial loss-weight temperatures, the weight loss was very slow (1–5%), which attributes to the water of samples. Thereafter, the rate of loss-weight became very intense. Loss- weight reactions were accompanied by nitrile cyclization reactions and interchain polymerization [123, 124].

As shown in Figure 6.1 The retain %weight for all precursors are close and about 30% at 1000 ˚C for all electrospun fibers with different precursors.

The secondary loss was due mainly to the degradation of the fibers. In the case of the stabilized fibers, it was found that there was a slight weight loss occurring at the early stage of measuring temperature. This can be ascribed to the removal of the chemical

groups formed on the fiber surfaces during the stabilization. Also, the webs heat-treated at 800 ˚C and at 1000 ˚C showed the initial weight loss of about 10%. This may be explained by that there were a number of different chemical species on the fiber surfaces in the webs and they were chemically and thermally unstable due to low carbonization temperature.

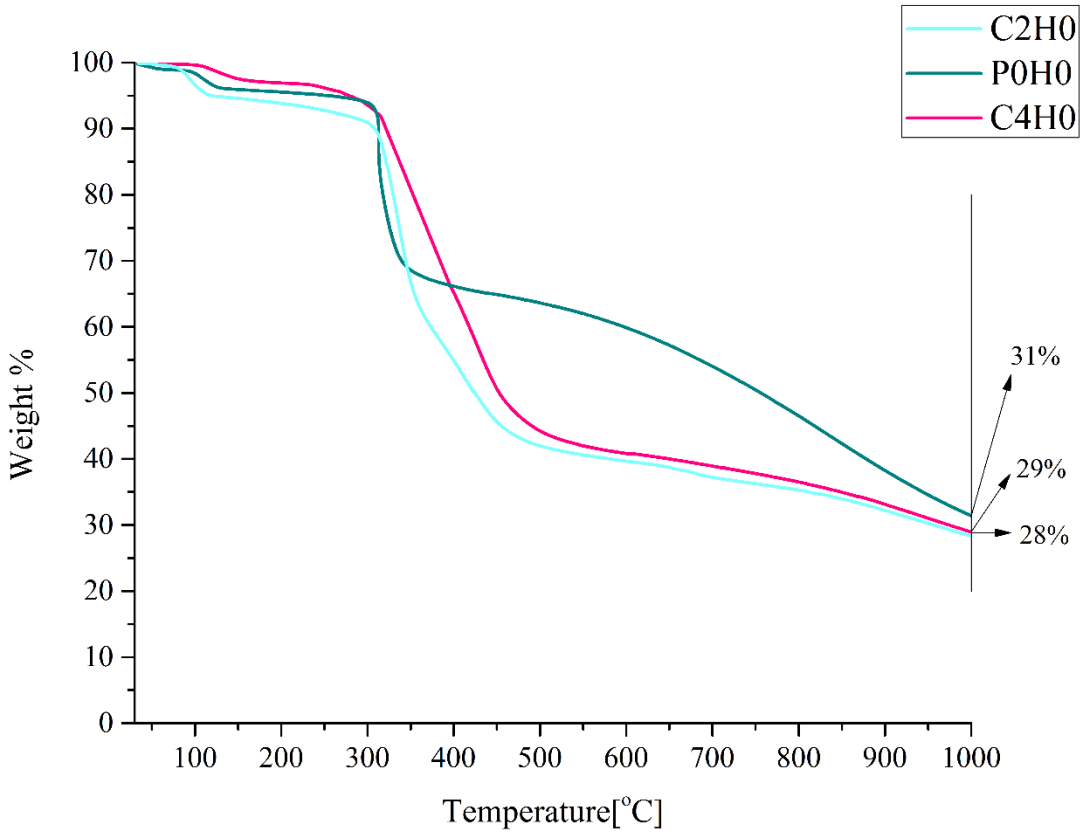

Figure 6.1: TGA thermograms of as-electrospun AN homopolymer and P(AN-co VAc), P(AN-co-IA) copolymers.

TGA thermogram of the fibers after oxidative stabilization process recorded as well. Figure 6.2 shown for the stabilized PAN, Poly(acrylonitrile-co-itaconic acid) and Poly(acrylonitrile-co-itaconic acid) nanofibers, this weight-loss peak started from about 300°C; when the temperature was increased to 450°C, about 24% of the weight was lost for P0S and C4S. Beyond 450°C, the weight decreased at a much slower rate, from 65 wt % at 450°C to 45 wt % at 800°C and to 30 wt % at 1000°C for C4S. For the stabilized PAN nanofibers, these numbers were about 52 and 34 wt % at 800 and 1000°C, respectively. Stabilized nanofibers which contain vinyl acetate represented nearly the same weight loss behaviour with P0S. These results are in good acoordance with previous studies [5].

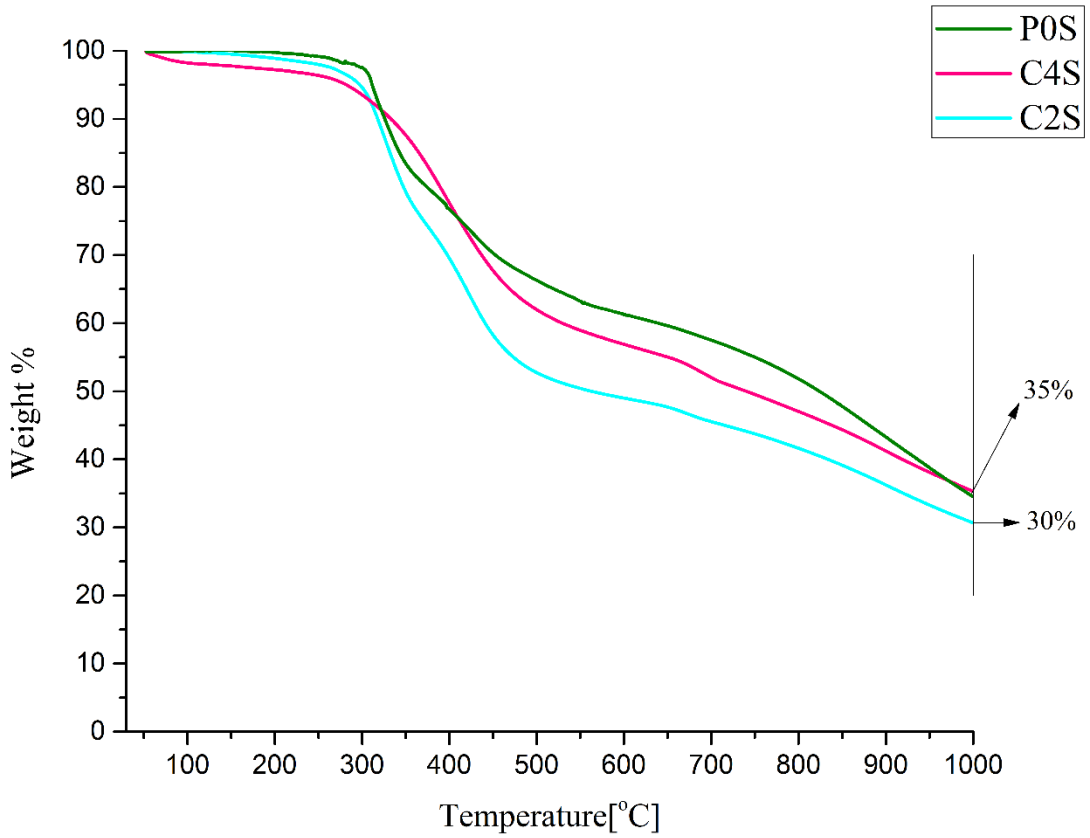

Figure 6.2: TGA thermograms of oxidative stabilized AN homopolymer and P(AN-co-VAc), P(AN-co-IA) copolymers.

With regard to the fact that high porous are prone to moisture adsorption, therefore unevitable weight loss occurred at about 100°C. Hence the relative wt % defined for show the weight loss except the moisture of material.

As shown in Figure 6.3 the loosing weight patern are about similar for all activated fibers. The relative sample weight % value which retain after the same TGA analysis regime are 70, 68 and 67 for (AN-co-IA), (AN-co-VAc) and AN homopolymer respectively at 1000°C. The results shown that using copolymers instead of homopolymer in precursor can improved the thermal stability of activated fibers opposes the thermal degradation.

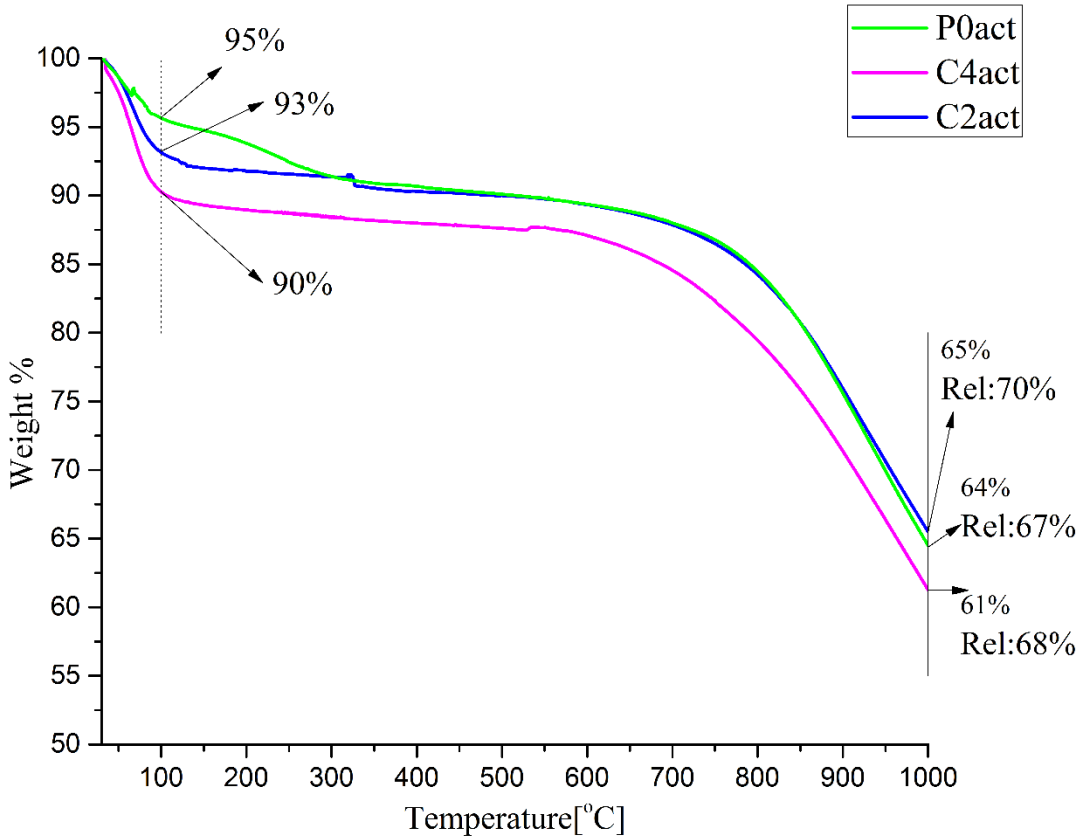

Figure 6.3: TGA thermograms of activated AN homopolymer and P(AN-co-VAc), P(AN-co-IA) copolymers.

Also The TGA results of the PAN, P(AN-co-VAc) and P(AN-co-IA) in electrospun, stabilization and activation modes are shown for each of them in the seprate plot to study on the effects of heating regim on each precursors in Figure 6.4, Figure 6.5 and Figure 6.6, respectively.

The TGA curves of the PAN nanofibers (Figure 6.4) show a dramatic weight loss between 300 and 400°C, which indicates the decomposition of PAN. About 30% of the weight was lost in this temperature range. For the stabilized PAN nanofibers, this weight-loss peak started from 300°C when the temperature was increased to 450°C, about 24% of the weight was lost. Beyond 450°C, the weight decreased at a much slower rate, from 65 wt % at 450°C to 45 wt % at 800°C and to 30 wt % at 1000°C. For the stabilized PAN nanofibers, these numbers were about 52 and 34 wt % at 800 and 1000°C, respectively. These results are in acoordance with previous studies [11].

As mentioned before for carbonized and activated fibers the “relative wt%” term defined. The TGA curve for the carbonized nanofibers indicates that only about 36 wt

% of the weight was lost at 1000°C. The activated sample showed similar weight loss patern to carbonized sample with this diffrence that after 650°C the weight loss rate in activated fibers is slower than carbonized fibers and the final weight loss is about 33% at 1000°C for activated PAN based CNFs.

During the complicated activation process, PAN generally goes through stabilization between 200°C and 400°C and carbonization at higher tempertures. Stabilization involves dehydrogenation, cyclization and, if it occurs in the air, oxidation. The exothermic process is due to the uncontrolled thermal polymerization of the nitrile group with the release of the heat of polymerization. During carbonization, the fibers lose non-carbon elements, as well as partial carbon, in the form of volatile byproduct gases, such as HCN, NH, and H. Finally, a graphite-like structure is formed. The initial heating of stabilized PAN fibers causes the growth of graphite-like ribbons by a dehydrogenation mechanism. Denitrogenation, which occurs as the temperature is increased, is responsible for the growth in the area and the transformation of these ribbons into thin, sheetlike structures and, at higher temperatures, for the bonding of adjacent sheets. These sheets contain numerous vacancy imperfections and are folded to enclose pencil-shaped voids oriented in the general direction of the fiber axis.

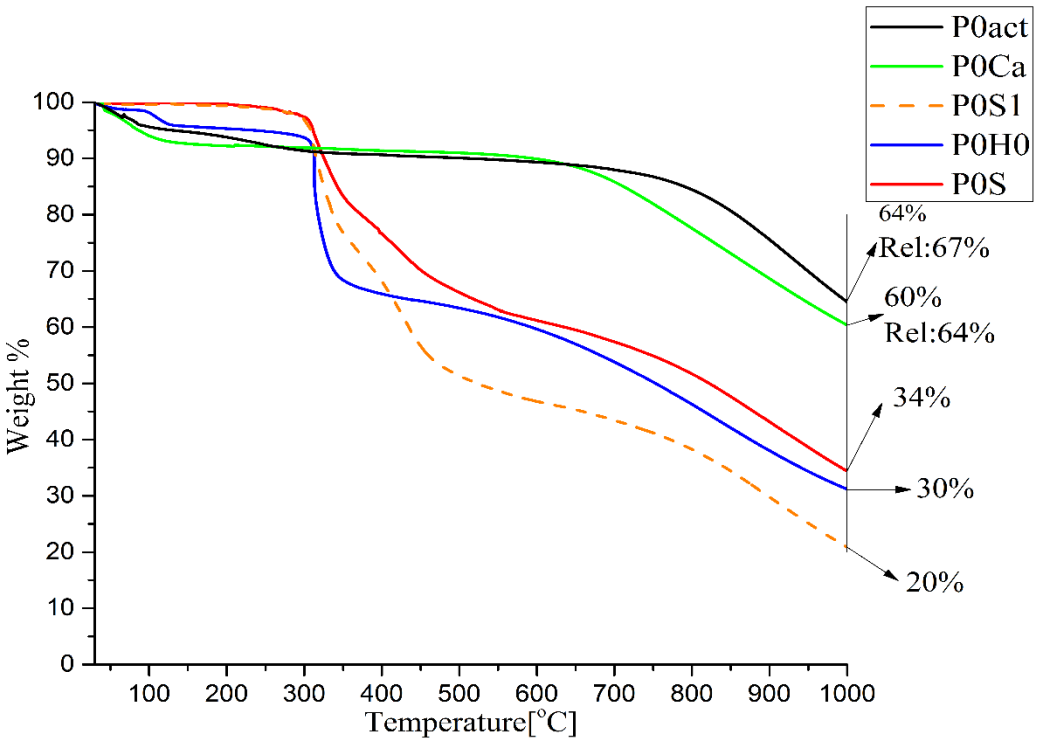

Figure 6.4: TGA thermograms of AN homopolymer based CNFs during the activation process.

As previously stated the thermal stability of copolymers was investigated by thermo-gravimetric analysis under N_2 atmosphere from 50°C to 1000°C at a heating rate of 10°C/min.

Thermal properties of electrospun P(AN-co-VAc) and P(AN-co-IA) nanofibers are investigated using TGA characterization. Figure 6.5 and Figure 6.6 depicted the TGA results of P(AN-co-VAc) and P(AN-co-IA) respectively.

Thermal properties of Electrospun, stabilized and activated fibers for each compolymers shown comparatively. Degradation temperature for stabilized fibers of P(AN-co-VAc) was about same as electrospun fibers with this diffrence that stabilized fibers lost its weight at slower rate than electrospun fibers. This behaviour is predictable because of dehydrogenation and cyclization occurred during oxidation and make the sample more resistant under the heat treatment.

Finally the stabilized sample weight retain 6% more than electrospun fibers which 29 wt% of sample preserved at 1000°C. this variance value diminished to 2% in P(AN-co-IA) electrospun and stabilized fiber at 1000°C which demonstrate that this specific stabilization heating regim is much appropriate for P(AN-co-VAc) in comparison with P(AN-co-IA).

Activated fibers in both samples show higher resistance against weight losing and once more its predictable because they had subjected to the heating regim which result to eliminate other elements during activation process.

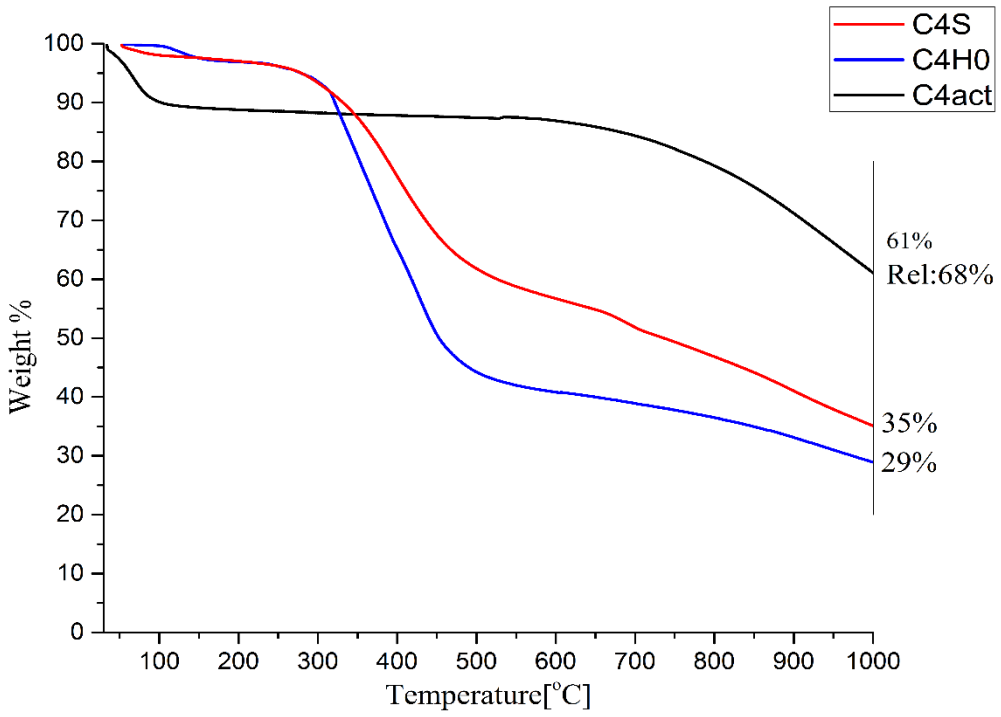

Figure 6.5: TGA thermograms of (AN-co-VAc) copolymer based CNFs during the activation process.

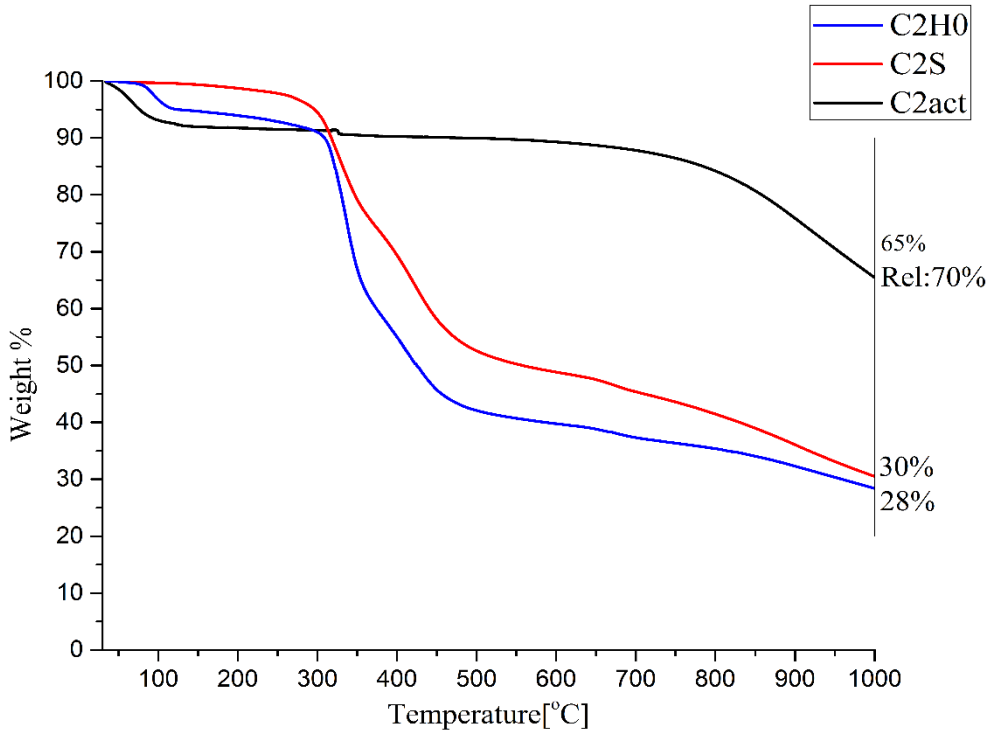

Figure 6.6: TGA thermograms of (AN-co-IA) copolymer based CNFs during the activation process.

6.2 Scanning electron microscopy of carbonized nanofibers

Figure 6.7 shows the surface morphologies by SEM of nanofibers which are oxidized with two different heating rate. (a,b) belong to AN homopolymer which is heating to the specific stabilization temperature (230°C) at heating rate 2°C/min while (c,d) represented the stabilized fibers which stabilized two time slower than the previous fibers at heating rate 1°C/min.

Faster heating regim provided fused fiber which is an indication of insufficient stabilization and the other indicate more better stabilization as can be seen in the Figure 6.7(c, d).

However, it was observed that PAN nanofibers had the tendency to become soft and stick to each other as a result of thermal stabilization. It was found that heating rate of 1 $^{\circ}C.min^{-1}$ during thermal stabilization reduced the sticking of fibers to a minimum. It is in concord with the literature [16, 48]

Figure 6.8 is other SEM image that illustrated activated carbon nano fiber which has drived from P(AN-co-IA)(85:15)%wt.

The pore formation after activation process observable evidently from the SEM images which is magnified to ×190,000.

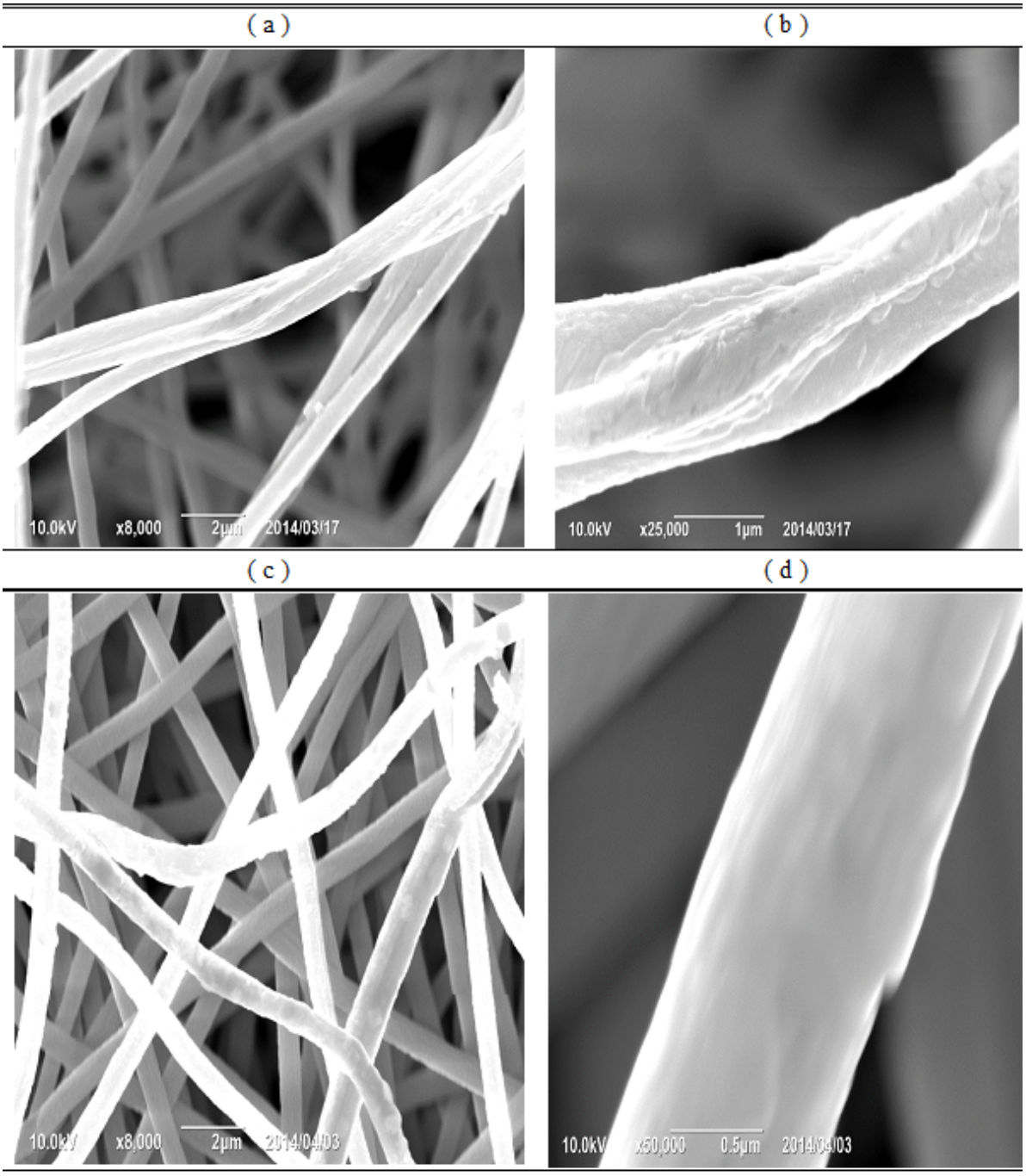

Figure 6.7:SEM micrograph of stabilized PAN nanofibers shown in different stabilization heating rate: (a and b) stabilization at heating rate 2°C/min, (c and d) stabilization at heating rate 1°C/min.

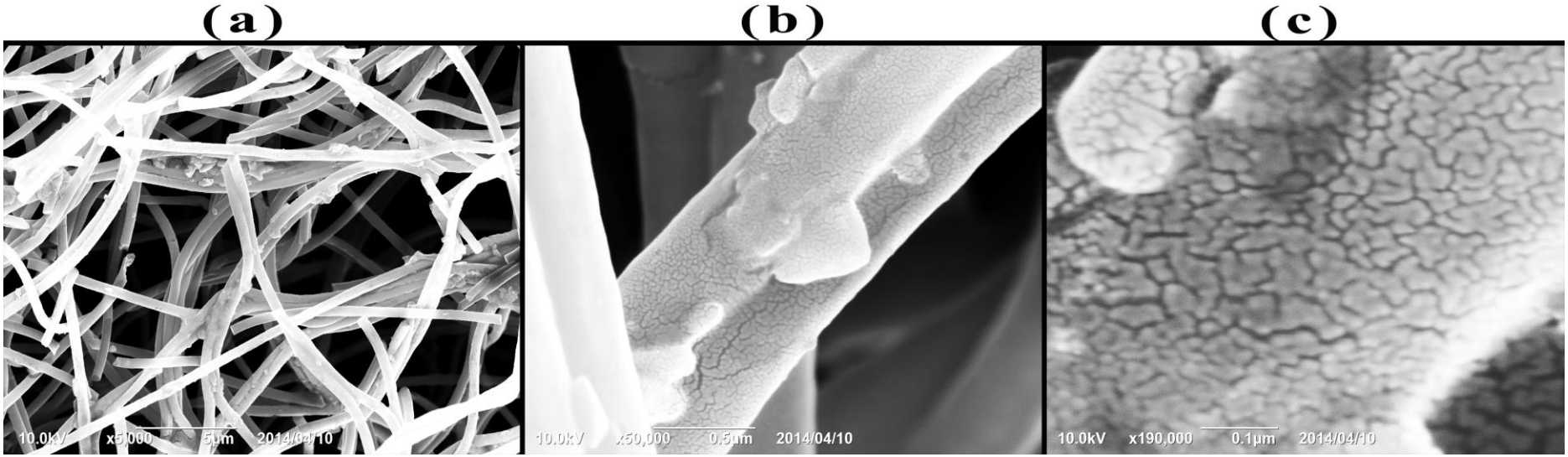

Figure 6.8: SEM micrograph of activated P(AN-co-IA) nanofibers shown in different scales: (a) ×2,000 magnification , (b) ×50,000 magnification, (c) ×190,000 magnification.

The fiber diameter distribution of AN homopolymer, (AN-co-IA) copolymer and (AN-co-VAc) copolymer provided in Figure 6.9. Fibers diameters in each step recorded(electrospun, stabilization, carbonization and activation).The diameters of fibers deacrease in stabilization and carbonization in compared with electrospun fibers due to shrinkage of the fibers which occurred during the heat treatment. This falling in the diameter size was sustained with mild slop for AN homopolymer after the activation. However for P(AN-co-IA) and P(AN-co-VAc) diameters raised up after the activation process had applied. Noticeably, activation is carried out to enlarge the diameters of the pores which are created during the carbonization process and to create some new porosity thus resulting in the formation of a well-developed and readily accessible pore structure with very large internal surface area.

Activated carbon fibers from P(AN-co-IA) copolymer was thicker than the activated carbon fibers from AN homopolymer precursor.

The diameter distribution data has collected from 700-800 fibers in average for each step of heat treatment during the activation process, also minimum, maximum, standard deviation, standard error and mean of the provided fiber diameter data has been shown in Figure 6.9. Measuring progression carried out by Image-Pro Plus software.

For Acrylonitrile homopolymer, electrospun fibers diameter was about 610 nm while during the specific heat treatment, after stabilization the fibers diameter drop to 580 nm and diameters for carbonized and activated form of fiber are about 450 and 350 nm respectively. As mentioned before, decreasing the fiber diameter was due to the shirinkage that result of evolving gases (burn off) occurring at high temperatures used during carbonization and activation.

The diameter value for P(AN-co-IA) in electrospun, oxidative stabilized, carbonized and activated fibers was about 510, 485, 345 and 440 nm respectively. However these values for P(AN-co-VAc) were 470, 355, 320 and 350 nm for electrospun, stabilized, carbonized and activated fibers.

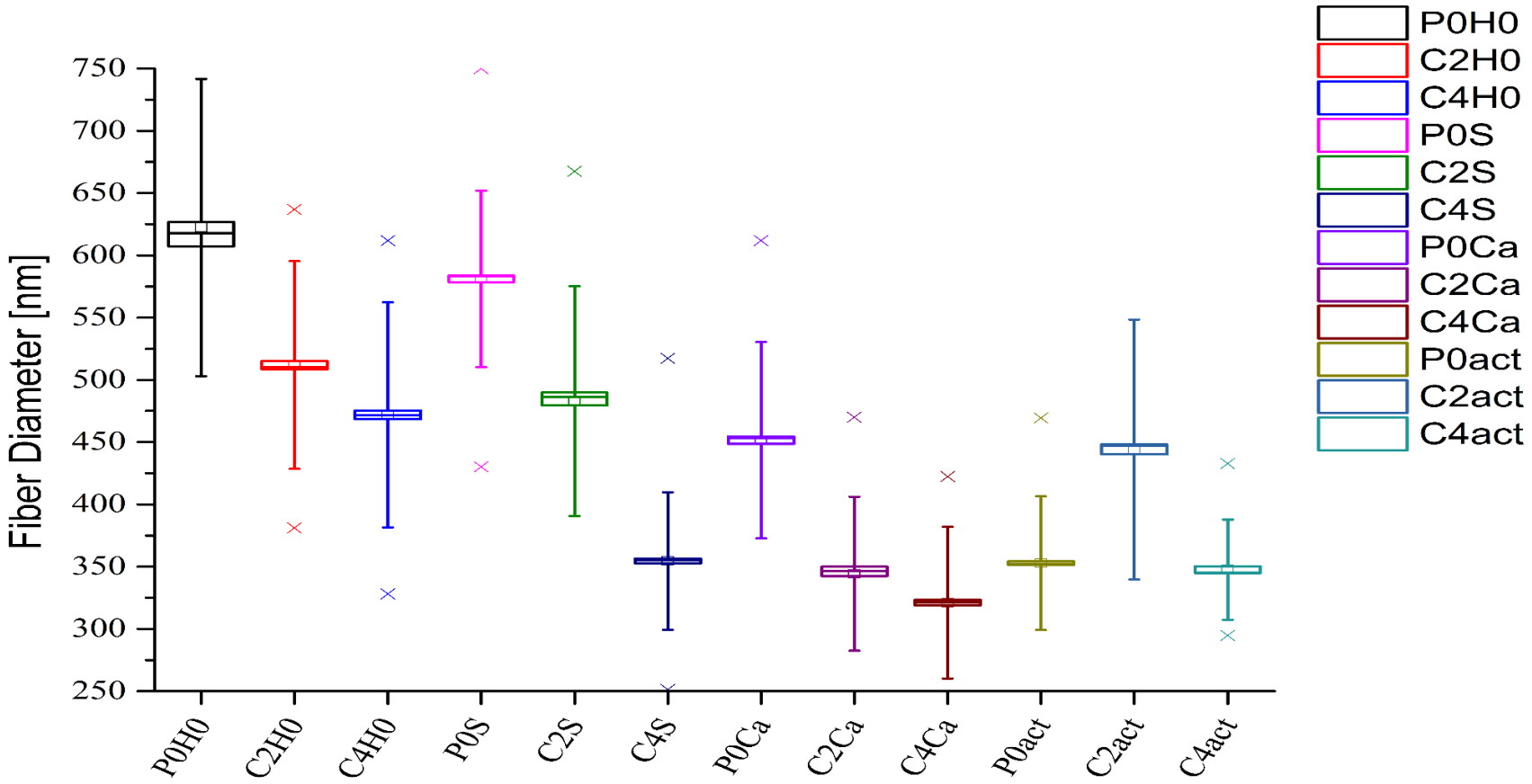

Figure 6.9: PAN Homopolymer, P(AN-co-IA) and P(AN-co-VAc) copolymers based carbon nanofibers diameter distributions during the activation process.

As the electrospun fiber diameter values shown, for the same electrospinning conditions for all of the precursors, diameter of the fibers with AN homopolymer precursor are more than copolymers. Using copolymers instead of AN homopolymers reduce the electrospun fibers diameter.

Owing to the fact that more fiber diameter lead to less surface area, it's noteworthy to mention that fibers diameter play crucial role in the surface area characteristics. The mean value of fiber diameter gathered in Table 6.2 that presented effect of different precursors on the fibers diameter.

The ratio of diameter change in beforehand and after the activation process for three different precursors of CNFs depicted in the last column of Table 6.2.

Table 6.2: Fibers diameters mean value.

Fibers	Electrospun Diameter	Stabilized Diameter	Carbonized Diameter(D_C)	Activated Diameter(D_A)	D_A/D_C
PAN	610 nm	580 nm	450 nm	350 nm	0.78
P(AN-co-IA)	510 nm	485 nm	345 nm	440 nm	1.28
P(AN-co-VAc)	470 nm	355 nm	320 nm	350 nm	1.09

With regard to the fact that the fibers diameter are the function of different terms such as all of the electrospinning conditions and effect of the particular heating regim to the electrospun fibers, and as mentioned before activation process carried out to enlarge the porosity diameter of the fibers, comparing the fibers diameter could given valued evidence about determining the most proper precursor which made more porosity extention during the activation process. As the last column of Table 6.2 the copolymer precursor which contained itaconic acid has the most porosity extention in this specified heat tratment and activation process. After that, P(AN-co-VAc) shown better efficiency than the acrylonitrile homopolymer.

6.3 Accelerated Surface Area and Porosimetry System

Due to the adsorption isotherms of nitrogen at 77.35 K contain a large amount of information on pore structure and accordingly their changes imply the alteration of pore structure, their measurements are the basis to estimate the pore structure parameters. So to characterize the porosity of final ACNFs, nitrogen adsorption isotherms (77 ◦K) were obtained using ASAP 2010, which was fully automatic.

Outgassing to a residual vacuum was carried out at 450˚C and 100˚C for ACNFs and electrospun nano-fibers respectly, for about 24 h.

As one of pore characteristic parameters, pore size distribution influences the equilibriums of adsorption and transport. Other parameters such as surface area, pore volume can be obtained from the information on pore size distribution such as t-plot.

Electrospun fibers and activated carbon nanofibers of three different precursor's porosity structure studied and recorded. BJH adsorption cumulative pore volume of pores and Pore diameters, maximum pore volume and median pore diameter of fibers obtained and the results represented in Table 6.3. According to Table **6.4** the samples BET surface area and micropore surface area analysed by using a Micromeritics ASAP 2010 (Accelerated Surface Area and Porosimetry System) as well [122].

Total pore volume was increased same as the result of BET specific surface area, comparing with electrospun fibers and activated fibers from 0.67 to 260 m^2/g about 400 times for acrylonitrile homopolymer fibers. BET surface area values for electrospun fibers augmented after activation form 3.46 to 375 m^2/g (about 110 times) and from 0.09 to 408 m^2/g (about 4500 time) for P(AN-co-IA) and P(AN-co-VAc) copolymers respectively. It demonstrated the gigantic effect of heating regim and activation process on the BET specific surface area of the fiber which deriven from acrylonitrile and vinyl acetate copolymers that could change 4500 time after the specific heat treatment.

As seen in Table 6.3, activated carbon with P(AN-co-IA) precursor demonstrated the highest value in "Barrett-Joyner-Halenda (BJH) adsorption cumulative pore volume of pores" and "average pore diameter" and after that P(AN-co-VAc) and AN homopolymer got placed respectively.

With regarding to the Table 6.2, Table 6.3 and Table **6.4** it's obvious that using copolymers instead of AN homopolymer could enhanced the surface and porosity characterization after activation process. In the matter of copolymer precursors, ACNFs with a smaller diameter shows a higher nitrogen adsorption. However the difference in the fiber diameters is much more than nitrogen adsorption variance value. Since the ACNFs with P(AN-co-IA) precursor shows better behaviour in comparison to P(AN-co-VAc) precursor in case of enlarging porosiy diameter during the

activation, it can be concluded that IA could be better choice as a copolymer with AN compared to VAc for surface area treatment. It's in agreement with literature [16, 54].

Table 6.3: Pore structure characterizing of the ACNFs and Electrospun Fibers.

Sample Code	BJH Adsorption CumulativePore Volume of pores[cm^3/g]	Average Pore Diameter[A]	Maximum Pore Volume[cm^3/g]	Median Pore Diameter[A]
P0H0	NA	NA	0.001904	10.1
C2H0	NA	NA	0.002122	18.9
C4H0	NA	NA	0.001454	19.3
P0act	0.008	13.34	0.12	8.9
C2act	0.036	26.22	0.19	7.6
C4act	0.011	18.62	0.20	8.6

Table 6.4: BET and Micropore surface area of the ACNFs and Electrospun fibers.

Sample Code	BET Surface area[m^2/g]	Micropore Surface Area[m^2/g]
P0H0	0.67	3
C2H0	3.46	4
C4H0	0.09	5
P0act	260	232
C2act	375	597
C4act	408	631

As mentioned before nitrogen adsorption isotherm is a standard tool for the characterization of porous materials especially carbonaceous adsorbents, providing invaluable information about the pore characteristics of adsorbents. According to International Union of Pure and Applied Chemistry (IUPAC), the pores of a porousmaterial can be classified into three groups [125] as follows:

(i) Micropores with a diameter of less than 2 nm.

(ii) Mesopores with a diameter between 2 and 50 nm.

(iii) Macropores with a diameter ofmore than 50 nm.

Figure 6.10 shows the nitrogen adsorption isotherms for ACNF samples from precursors of two copolymer of acrylonitrile as well as PAN nano fibers after CO_2 activation at 750˚C for 1 hour (as explained in the Experimental section).

According to the IUPAC, the long plateau of curves in Figure 6.10 basically indicates the adsorption characteristics of microporous (type I) adsorbents. It seems that to all intents and purposes, it is the micropores that dominated the scene. However, although the increase in the slope at the end of the isotherms (over relative pressure 0.95) for C2act and C4act samples may imply the presence of some mesopores characteristics, it is probable that parameters such as widening of the distribution of the micropores to values over 1 nm or increased roughness of the external areas have led to the slope increase. So AN copolymer activated carbon fibers base, have micro- and mesopores. Also small amounts of capillary condensation (macropores) at the points of contact of the fibers cannot be ruled out [48].

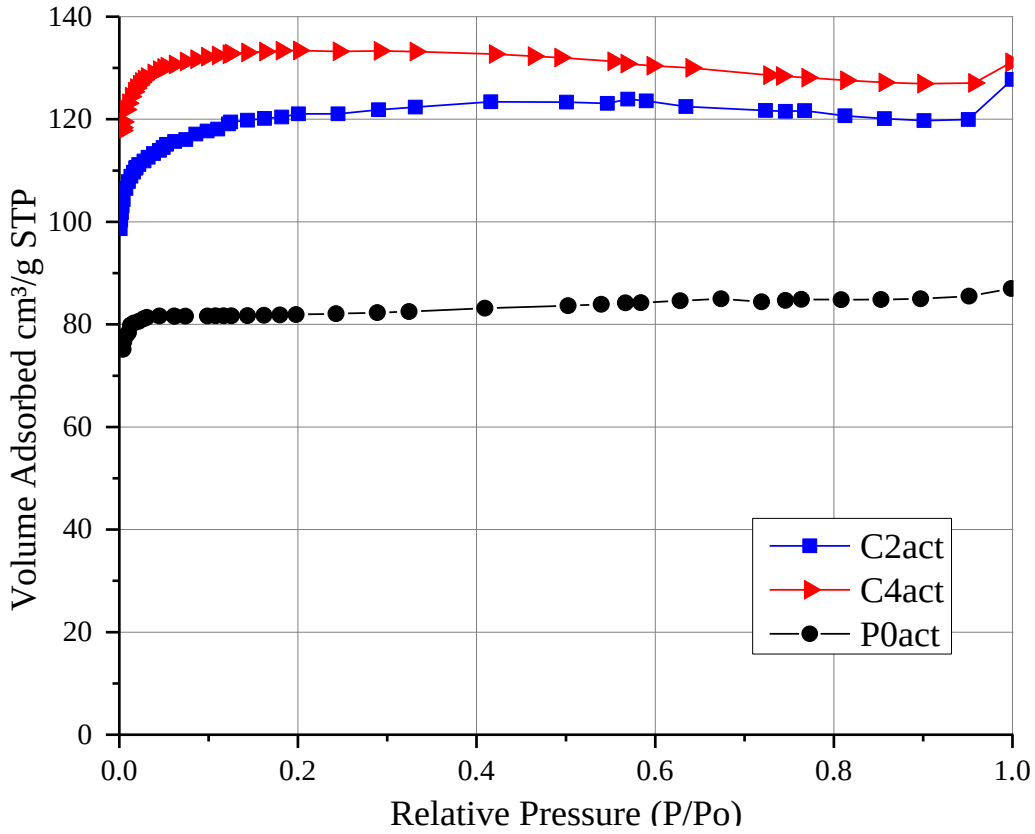

Figure 6.10: Nitrogen adsorption isotherms of activated fibers.

6.4 Fourier transform infrared spectroscopy– attenuated total reflectance (FTIR-ATR)

The synthesized AN homopolymer, P(AN-co-VAc) and P(AN-co-IA) copolymers are characterized spectroscopically by FTIR-ATR. As shown in Figure 6.11 PAN shows

its characteristic absorption peaks at 2243 cm-1 and 1451 cm^{-1}, corresponding to CN stretching and CH bending, respectively [30].

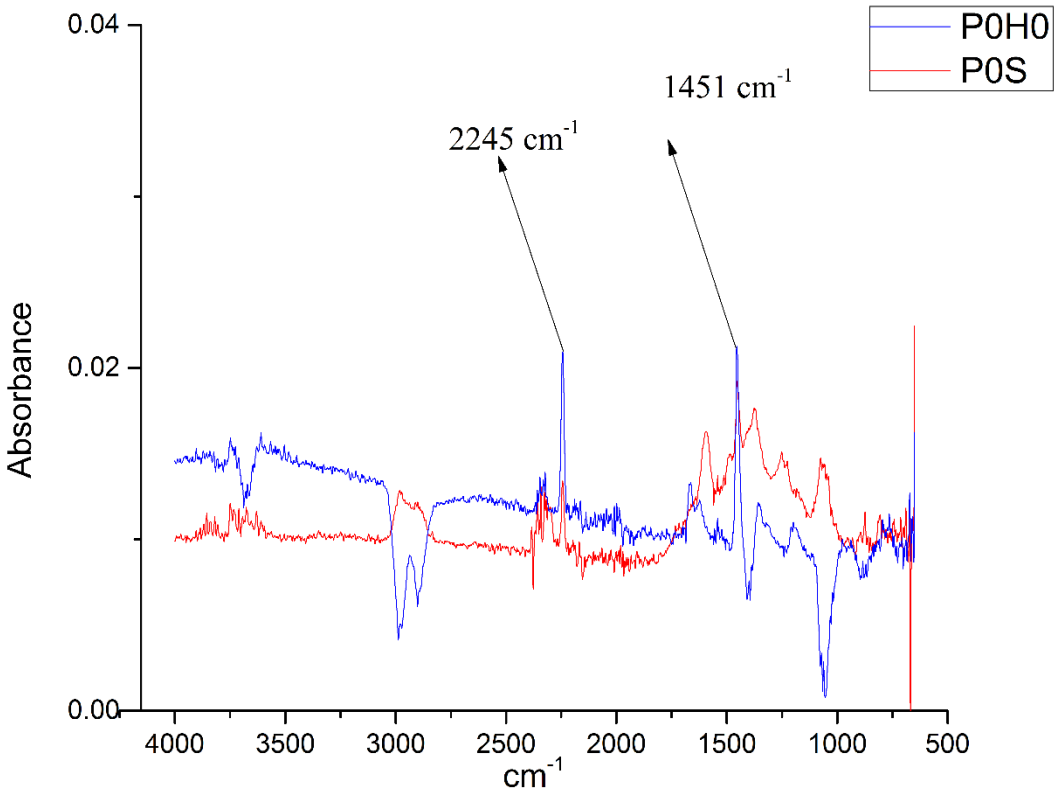

Figure 6.11: FTIR–ATR spectra of nano fibers based on P(AN-co-IA) copolymer (as-electrospun and stabilized nanofibers).

For P(AN-co-IA), the C-C streching peaks can be observed at 1668 cm^{-1} for IA as depicted in Figure 6.12. Also strong peak around 1450 cm^{-1} indicates the presence of methylene groups (CH_2) in our as-electrospun fibers. The peaks appeared at relevant plot at 1096 cm^{-1} and 1235 cm^{-1} represented C-O-C function of ether and ester and also1738 cm^{-1} which represent C=O vibration of ester function for the copolymer which contained itaconic acid. The peak at 2243 cm^{-1} depicted due to C≡N streching. This peak subsided after oxidative stabilization due to the cyclization process and changing the C≡N bonds to C=N.

The other peaks which mentioned above lessened as well due to the effect of heat treatment of stabilization step.

The absorption bands of 2976 cm^{-1} is attributed to -CH2 streching and bending peaks. The peak at 2890 $cm^{-1}$and 873 cm^{-1} is related to -CH peak of acrylonitrile units [30].

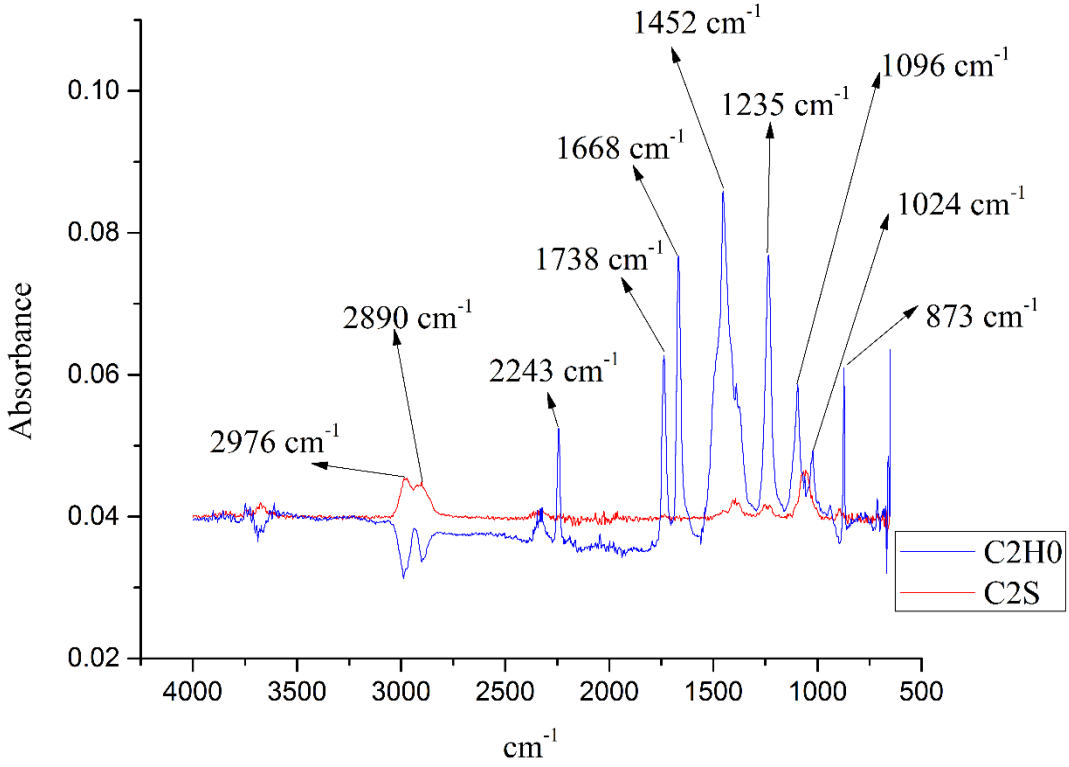

Figure 6.12: FTIR–ATR spectra of nano fibers based on P(AN-co-IA) copolymer. (as-electrospun and stabilized nanofibers).

The C=O, and C-O stretching vibration peaks can be observed at 1719 and 1065 cm^{-1}, respectively, for PVAc as illustrated in Figure 6.13.

The strong absorption bands for P(AN-co-VAc) are C=O stretching (1719 cm^{-1}) and CN stretching (2243 cm^{-1}) [8, 126]. These results are in good agreement with literature.

The absorption bands of 2975 cm^{-1} is endorsed $–CH_2$ streching and bending peaks. Also the peak at 2890 cm^{-1} is related to -CH peak of acrylonitrile units [23] [127].

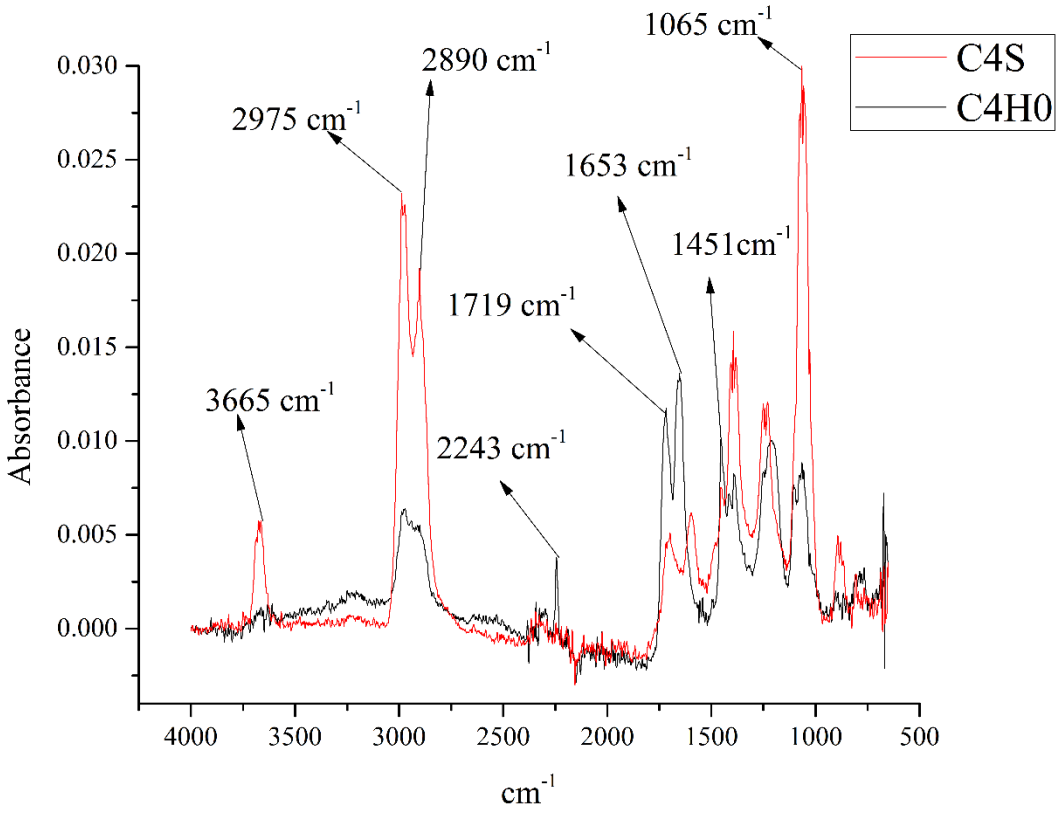

Figure 6.13: FTIR–ATR spectra of nano fibers based on P(AN-co-VAc) copolymer. (as-electrospun and stabilized nanofibers).

Figure 6.14 presents the relation between absorbance ratio of characteristic VAc peaks to AN and VAc and also IA peaks in FTIR ATR spectrums. The ratio of the absorbance of C=O stretching band at 1738 cm^{-1} to the total absorbance of CN stretching band at 2243 cm^{-1} and C=O stretching band at 1738 cm^{-1} was obtained from FTIR–ATR [5].

The most prominent structural changes were the decrease in the intensities of the 2243–2241 cm^{-1}, attributed to C≡N band, and the decrease of those for aliphatic C–H ones and the decrease of the 1668 cm^{-1} amide band, attendant with the advent and increase of a shoulder-like peak in 1719 cm^{-1} (due to cyclic C=O), the band at 1568 cm^{-1} (due to C=N,C=C,N–H mixed), and the band in 873 cm^{-1} (due to C=C–H) [128].

Figure 6.15 illustrate spectrums of oxidized fibers from different precursors comparingly. These spectroscopic results have shown that some chemical processes occurred in the stages of preoxidation. Firstly, reaction of nitriles results in conjugated C=N containing structures which result from intramolecular cyclization or intermolecular crosslinking.

Secondly, the generation of conjugated C=C structures results from dehydrogenation or from imine-enamine tautomerization and subsequent isomerization [129]. Thirdly, oxidation gives rise to carbonyl groups [130].

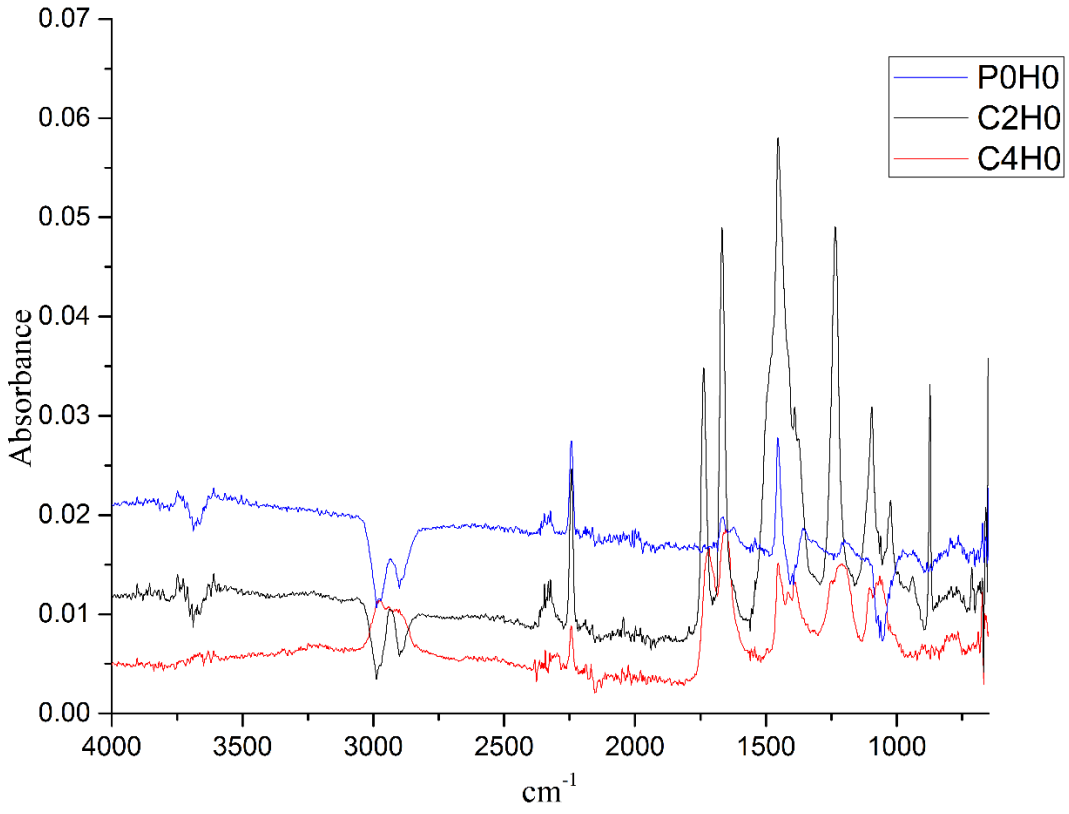

Figure 6.14: FTIR–ATR spectra of as-electrospun nano fibers based on AN homopolymer and P(AN-co-IA), P(AN-co-VAc) copolymers.

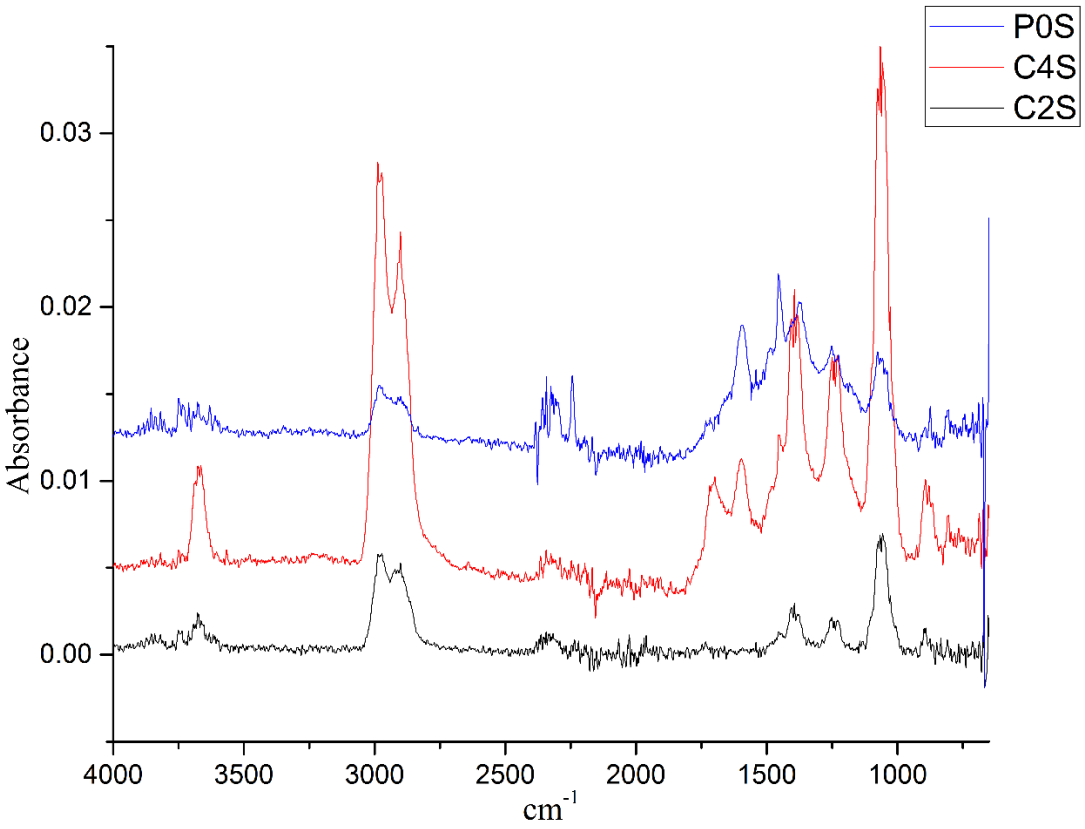

Figure 6.15: FTIR–ATR spectra of oxidative stabilized carbon nano fibers based on different polymers.

7. CONCLUSION

- Regarding to the TGA results, thermal stability of PAN is improved after being copolymerized with VAc, and thus confirming the effect of VAc and IA functional groups existed in copolymers in addition to nitrile groups of PAN.
- The TGA, SEM images and FTIR results confirming that the stabilization process carried out with the chosen heating regime for all three polymeric precursors.
- Fused carbon fibers obtained from PAN homopolymer precursor due to two time increasing the stabilization heating rate. Indicating insufficient stabilization.
- At the same electrospinning parameters, PAN homopolymer based as-electrospun fibers showed higher fiber diameter in comparison with other two copolymers.
- The carbon fibers with IA precursor, demonstrated more extension in the diameter between the carbonization and activation process.
- BET surface area values for electrospun fibers augmented after activation form 3.46 to 375 m2/g (about 110 times) and from 0.09 to 408 m2/g (about 4500 time) for P(AN-co-IA) and P(AN-co-VAc) copolymers respectively.
- P(AN-co-Vac) and P(AN-co-IA) showed close behavior(such as BET surface area after activation) in our specific heat treatment, it could be concluded that the weaken mechanical properties of the fibers with VAc is the main reason of inapplicability of these fibers in compare with IA.
- For all ACNFs It is the micropores that dominated the scene. However, although the increase in the slope at the end of the isotherms (over relative pressure 0.95) for C2act and C4act samples may imply the presence of some mesopores characteristics.

REFERENCES

[1] **Edwards, I. A., Marsh, H., Menendez, R., Rand, B., West, S., Hosty, A., Gray, R.** (1989). *Introduction to carbon science*. *(H. Marsh, Ed.)*. London: Butterworth.

[2] **Zussman, E., Chen, X., Ding, W., Calabri, L., Dikin, D. a., Quintana, J. P., & Ruoff, R. S.** (2005). Mechanical and structural characterization of electrospun PAN-derived carbon nanofibers. *Carbon*, *43*(10), 2175–2185.

[3] **Xiang, W., Yulan, L., & Limin, W.** (2010). Characterization of copolymerization of acrylonitrile with the functionalized comonomers in dimethyl sulfoxide solvent and copolymers suitable for carbon fibers. *E-Polymers*, (135), 1–12.

[4] **Saufi, S., & Ismail, A.** (2002). Development and characterization of polyacrylonitrile (PAN) based carbon hollow fiber membrane. *Songklanakarin Journal of Science and Technology*, (January 2003).

[5] **Cetiner, S., Sen, S., Arman, B., & Sarac, a. S.** (2013). Acrylonitrile/vinyl acetate copolymer nanofibers with different vinylacetate content. *Journal of Applied Polymer Science*, *127*(5), 3830–3838.

[6] **Debuigne, A., Warnant, J., Jérôme, R., Voets, I., de Keizer, A., Cohen Stuart, M. A., & Detrembleur, C.** (2008). Synthesis of Novel Well-Defined Poly(vinyl acetate)- b -poly(acrylonitrile) and Derivatized Water-Soluble Poly(vinyl alcohol)- b -poly(acrylic acid) Block Copolymers by Cobalt-Mediated Radical Polymerization. *Macromolecules*, *41*(7), 2353–2360.

[7] **Mayo, F. R., Walling, C., Lewis, F. M., & Hulse, W. F.** (1948). Copolymerization. V. 1 Some Copolymerizations of Vinyl Acetate. *Journal of the American Chemical Society*, *70*(4), 1523–1525.

[8] **Cetiner, S., Kalaoglu, F., Karakas, H., & Sarac, A. S.** (2011). Dielectric, FTIR spectroscopic and atomic force microscopic studies on polypyrrole-poly(acrylonitrile-co-vinyl acetate) composites. *Polymer Composites*, *32*(4), 546–557.

[9] **Zhou, Z., Lai, C., Zhang, L., Qian, Y., Hou, H., Reneker, D. H., & Fong, H.** (2009). Development of carbon nanofibers from aligned electrospun polyacrylonitrile nanofiber bundles and characterization of their microstructural, electrical, and mechanical properties. *Polymer*, *50*(13), 2999–3006.

[10] **Pashaloo, F., Bazgir, S., & Tamizifar, M.** (2009). Preparation and characterization of carbon nanofibers via electrospun PAN nanofibers. *Textile Science and Technology Journal*, *3*(2).

[11] **Agend, F., Naderi, N., & Fareghi-Alamdari, R.** (2007). Fabrication and electrical characterization of electrospun polyacrylonitrile-derived carbon nanofibers. *Journal of Applied Polymer Science*, *106*(1), 255–259.

[12] **Rahaman, M. S. a., Ismail, A. F., & Mustafa, A.** (2007). A review of heat treatment on polyacrylonitrile fiber. *Polymer Degradation and Stability*, *92*(8), 1421–1432.

[13] **Edie, D. D.** (1998). The effect of processing on the structure and properties of carbon fibers. *Carbon*, *36*(4), 345–362.

[14] **Ko, T.-H.** (1991). Influence of continuous stabilization on the physical properties and microstructure of PAN-based carbon fibers. *Journal of Applied Polymer Science*, *42*(7), 1949–1957.

[15] **Shokuhfar, a., Sedghi, A., & Farsani, R. E.** (2006). Effect of thermal characteristics of commercial and special polyacrylonitrile fibres on the fabrication of carbon fibres. *Materials Science and Technology*, *22*(10), 1235–1239.

[16] **Yusof, N., & Ismail, A. F.** (2012). Post spinning and pyrolysis processes of polyacrylonitrile (PAN)-based carbon fiber and activated carbon fiber: A review. *Journal of Analytical and Applied Pyrolysis*, *93*, 1–13.

[17] **Chen, J. ., & Harrison, I. .** (2002). Modification of polyacrylonitrile (PAN) carbon fiber precursor via post-spinning plasticization and stretching in dimethyl formamide (DMF). *Carbon*, *40*(1), 25–45.

[18] **Houtz, R. C.** (1950). "Orlon" Acrylic Fiber: Chemistry and Properties. *Textile Research Journal*, *20*(11), 786–801.

[19] **Standage, A., & Matkowsky, R.** (1971). Thermal oxidation of polyacrylonitrile. *European Polymer Journal*, *7*(September 1970), 775–783.

[20] **Friedlander, H., Jr, L. P., Brandrup, J., & Kirby, J. R.** (1968). On the chromophore of polyacrylonitrile. VI. Mechanism of color formation in polyacrylonitrile. *Macromolecules*, *I*(1), 79–86.

[21] **Watt, W., & Johnson, W.** (1975). Mechanism of oxidisation of polyacrylonitrile fibres. *Nature*, *257*, 210–212.

[22] **Grassie, N., Hay, J. N., & McNeill, I. C.** (1958). Coloration in acrylonitrile and methacrylonitrile polymers. *Journal of Polymer Science*, *31*(122), 205–206.

[23] **Burlant, W. J., & Parsons, J. L.** (1956). Pyrolysis of polyacrylonitrile. *Journal of Polymer Science*, *22*(101), 249–256.

[24] **La Combe, E. M.** (1957). Color formation in polyacrylonitrile. *Journal of Polymer Science*, *24*(105), 152–154.

[25] **Coleman, M. M., & Petcavich, R. J.** (1978). Fourier transform infrared studies on the thermal degradation of polyacrylonitrile. *Journal of Polymer Science: Polymer Physics Edition*, *16*(5), 821–832.

[26] **Fochler, H. S., Mooney, J. R., Ball, L. E., Boyer, R. D., & Grasselli, J. G.** (1985). Infrared and NMR spectroscopic studies of the thermal degradation of polyacrylonitrile. *Spectrochimica Acta Part A: Molecular Spectroscopy*, *41*(1), 275–278.

[27] **Xue, T. J., McKinney, M. A., & Wilkie, C. A.** (1997). The thermal degradation of polyacrylonitrile. *Polymer Degradation and Stability*, *58*(1), 193–202.

[28] **Gupta, a., & Harrison, I. R.** (1997). New aspects in the oxidative stabilization of PAN-based carbon fibers: II. *Carbon*, *35*(6), 809–818.

[29] **Bajaj, P., Sreekumar, T. ., & Sen, K.** (2001). Thermal behaviour of acrylonitrile copolymers having methacrylic and itaconic acid comonomers. *Polymer*, *42*(4), 1707–1718.

[30] **Ouyang, Q., Cheng, L., Wang, H., & Li, K.** (2008). Mechanism and kinetics of the stabilization reactions of itaconic acid-modified polyacrylonitrile. *Polymer Degradation and Stability*, *93*(8), 1415–1421.

[31] **Dunham, M., & Edie, D.** (1992). Model of stabilization for pan-based carbon fiber precursor bundles. *Carbon*, *30*(3), 435–450.

[32] **Zhang, W., Jie, L., & Liang, J.** (2004). New evaluation on the preoxidation extent of different PAN precursors. *Journal of materials science and technology*, *20*(4), 369–372.

[33] **Yu, M., Wang, C., & Bai, Y.** (2008). Effect of oxygen uptake and aromatization on the skin–core morphology during the oxidative stabilization of polyacrylonitrile fibers. *Journal of Applied Polymer Science*, *107*, 1939–1945.

[34] **Yu, M., Wang, C., Bai, Y., Wang, Y., & Zhu, B.** (2006). Evolution of tension during the thermal stabilization of polyacrylonitrile fibers under different parameters. *Journal of Applied Polymer Science*, *102*(6), 5500–5506.

[35] **Yu, M., Wang, C., Bai, Y., Wang, Y., Wang, Q., & Liu, H.** (2006). Combined Effect of Processing Parameters on Thermal Stabilization of PAN Fibers. *Polymer Bulletin*, *57*(4), 525–533.

[36] **Yu, M.-J., Bai, Y.-J., Wang, C.-G., Xu, Y., & Guo, P.-Z.** (2007). A new method for the evaluation of stabilization index of polyacrylonitrile fibers. *Materials Letters*, *61*(11-12), 2292–2294.

[37] **Hou, Y., Sun, T., Wang, H., & Wu, D.** (2008). A new method for the kinetic study of cyclization reaction during stabilization of polyacrylonitrile fibers. *Journal of Materials Science*, *43*(14), 4910–4914.

[38] **Mathur, R. B., Dhami, T. L., & Bahl, O. P.** (1986). Shrinkage behaviour of modified PAN precursors—Its influence on the properties of resulting carbon fibre. *Polymer Degradation and Stability*, *14*(2), 179–187.

[39] **Cui, C., Yu, L., & Wang, C.** (2010). The degradation and prestabilization of acrylonitrile copolymers. *Journal of Applied Polymer Science*, *117*, 1596–1600.

[40] **Fitzer, E., & Müller, D.** (1975). The influence of oxygen on the chemical reactions during stabilization of PAN as carbon fiber precursor. *Carbon*, *13*(Formula 4), 63–69.

[41] **Ge, H., Liu, H., Chen, J., & Wang, C.** (2009). The microstructure of polyacrylonitrile- stabilized fibers. *Journal of Applied Polymer Science*, *113*, 2413–2417.

[42] **He, D.-X., Wang, C.-G., Bai, Y.-J., Lun, N., Zhu, B., & Wang, Y.-X.** (2007). Microstructural evolution during thermal stabilization of PAN fibers. *Journal of Materials Science*, *42*(17), 7402–7407.

[43] **Cho, C.-W., Cho, D.-H., Ko, Y.-G., Kwon, O.-H., & Kang, I.-K.** (2007). Stabilization, Carbonization, and Characterization of PAN Precursor Webs Processed by Electrospinning Technique. *Carbon letters*, *8*(4), 313–320.

[44] **Fitzer, E., & Frohs, W.** (1986). Optimization of stabilization and treatment of PAN fibres and structural of the resulting carbon fibres. *Carbon*, *24*(4), 387–395.

[45] **Hou, Y., Sun, T., Wang, H., & Wu, D.** (2008). Effect of Heating Rate on the Chemical Reaction during Stabilization of Polyacrylonitrile Fibers. *Textile Research Journal*, *78*(9), 806–811.

[46] **Wu, G., Lu, C., Ling, L., Hao, A., & He, F.** (2005). Influence of tension on the oxidative stabilization process of polyacrylonitrile fibers. *Journal of Applied Polymer Science*, *96*(4), 1029–1034.

[47] **Fazlitdinova, A. G., Tyumentsev, V. A., Podkopayev, S. A., & Shveikin, G. P.** (2010). Changes of polyacrylonitrile fiber fine structure during thermal stabilization. *Journal of Materials Science*, *45*(15), 3998–4005.

[48] **Tavanai, H., Jalili, R., & Morshed, M.** (2009). Effects of fiber diameter and CO 2 activation temperature on the pore characteristics of polyacrylonitrile based activated carbon nanofibers. *Surface and Interface Analysis*, *41*(10), 814–819.

[49] **Wang, G., Pan, C., Wang, L., Dong, Q., Yu, C., Zhao, Z., & Qiu, J.** (2012). Activated carbon nanofiber webs made by electrospinning for capacitive deionization. *Electrochimica Acta*, *69*, 65–70.

[50] **Lee, K. J., Shiratori, N., Lee, G. H., Miyawaki, J., Mochida, I., Yoon, S.-H., & Jang, J.** (2010). Activated carbon nanofiber produced from electrospun polyacrylonitrile nanofiber as a highly efficient formaldehyde adsorbent. *Carbon*, *48*(15), 4248–4255.

[51] **Datsyuk, V., Kalyva, M., Papagelis, K., Parthenios, J., Tasis, D., Siokou, A., … Galiotis, C.** (2008). Chemical oxidation of multiwalled carbon nanotubes. *Carbon*, *46*(6), 833–840.

[52] **Mathur, R., Bahl, O., & Mittal, J.** (1992). A new approach to thermal stabilisation of PAN fibres. *Carbon*, *30*(4).

[53] **Bromley, J.** (1971). Gas evolution processes during the formation of carbon fibers. In The Plastics Institute. *In International conference on carbon fibers, their composites and applications.* (pp. 3–9). London, England: The Plastics Institute .

[54] **Morgan, P.** (2005). *Carbon fibers and their composites* (pp. 121–146, 200–235, 255–260). Boca Raton: taylor & francis.

[55] **Marsh, H., & Rodriguez-reinoso, F.** (2006). *Activated Carbon*. *(H. Marsh & F. Rodriguez-reinoso, Eds.)*. Elsevier Science & Technology Books.

[56] **Kyotani, T.** (2000). Control of pore structure in carbon. *Carbon*, *38*(2), 269–286.

[57] **Figueiredo, J., Pereira, M., Freitas, M., & Orfao, J.** (1999). Modification of the surface chemistry of activated carbons. *Carbon*, *37*, 1379–1389.

[58] **Xiu, G., & Li, P.** (2000). Prediction of breakthrough curves for adsorption of lead(II) on activated carbon fibers in a fixed bed. *Carbon*, *38*(7), 975–981.

[59] **Lewis, C., I., & T., R.** (1988). Carbonaceous mesophase: History and prospects. *Carbon*, *26*(5), 757–758.

[60] **Donnet, B., J., Bansal, & C., R.** (1984). Carbon Fibers International Fiber Science & Technology Series.

[61] **Tuakta, C.** (2005). *Use of fiber reinforced polymer composite in bridge structures*. Massachusetts Institute of Technology.

[62] **Chung, D.** (1994). *Carbon fiber composites*. Butterworth-Heinemann.

[63] **Kobets, L. P., & Deev, I. S.** (1998). Carbon fibres: Structure and mechanical properties. *Composites Science and Technology*, *57*(12), 1571–1580.

[64] **Peebles Jr, L. H.** (1994). Carbon fibres: structure and mechanical properties. *International materials reviews*, *39*(2), 75–92.

[65] **Figueiredo, J. L., Bernardo, C. A., Baker, R. T. K., & Hüttinger, K. J.** (1989). Carbon fibers filaments and composites. *springer*, (177).

[66] **Rand, B., & Shepherd, P. M.** (1980). Glass transformations in some pitch materials. *Fuel*, *59*(11), 814–816.

[67] **Zander, M.** (1987). On the composition of pitches. *Fuel*, *66*(11), 1536–1539.

[68] **Milewski, J. V., & Katz, H. S.** (1987). *Handbook of reinforcements for plastics*. Van Nostrand Reinhold Company.

[69] **Marsh, H., Heintz, E. A., & Rodriguez-reinoso, F.** (1997). *Carbon Materials: An Overview of Carbon Artifacts*. *(H. Marsh, E. A. Heintz, & F. Rodriguez-reinoso, Eds.)*. spain: University of Alicante Secretariado de Publicationes.

[70] **Tibbetts, G. G.** (1989). Vapor-grown carbon fibers: status and prospects. *Carbon*, *27*(5), 745–747.

[71] **Katsuki, H., Matsunaga, K., Egashira, M., & Kawasumi, S.** (1981). Formation of carbon fibers from naphthalene on some sulfur-containing substrates. *Carbon*, *19*(2), 148–150.

[72] **Ram, M. J.** (1972). U.S. Patent No. 3,657,409. U. S. Washington, DC.

[73] **Ahn, Y. C., Park, S. K., Kim, G. T., Hwang, Y. J., Lee, C. G., Shin, H. S., & Lee, J. K.** (2006). Development of high efficiency nanofilters made of nanofibers. *Current Applied Physics*, *6*(6), 1030–1035.

[74] **Lannutti, J., Reneker, D., Ma, T. E. A., Tomasko, D., & Farson, D.** (2007). Electrospinning for tissue engineering scaffolds. : C, 27(3), 504-509. *Materials Science and Engineering*, *27*(3), 504–509.

[75] **Hunley, M. T., & Long, T. E.** (2008). Electrospinning functional nanoscale fibers: a perspective for the future. Polymer International, 57(3), 385-389. *polymer international*, *57*(3), 385–389.

[76] **Reneker, D. H., & Yarin, A. L.** (2008). Electrospinning jets and polymer nanofibers. *Polymer*, *49*(10), 2387–2425.

[77] **Zussman, E., Theron, A., & Yarin, A. L.** (2003). Formation of nanofiber crossbars in electrospinning. *Applied physics letters*, *82*(6), 973–975.

[78] **He, J. H., Wan, Y. Q., & Yu, J. Y.** (2005). Scaling law in electrospinning: relationship between electric current and solution flow rate. *Polymer*, *46*(8), 2799–2801.

[79] **Zeleny, J.** (1914). The electrical discharge from liquid points, and a hydrostatic method of measuring the electric intensity at their surfaces. *physical review*, *3*(2), 69.

[80] **Taylor, G.** (1969). Electrically driven jets. *Proceedings of the Royal Society of London. A. Mathematical and Physical Sciences*, *313*(1515), 453–475.

[81] **Huang, Z.-M., Zhang, Y.-Z., Kotaki, M., & Ramakrishna, S.** (2003). A review on polymer nanofibers by electrospinning and their applications in nanocomposites. *Composites Science and Technology*, *63*(15), 2223–2253.

[82] **Bhardwaj, N., & Kundu, S. C.** (2010). Electrospinning: a fascinating fiber fabrication technique. *Biotechnology advances*, *28*(3), 325–47. doi:10.1016/j.biotechadv.2010.01.004

[83] **Kidoaki, S., Kwon, I. K., & Matsuda, T.** (2005). Mesoscopic spatial designs of nano-and microfiber meshes for tissue-engineering matrix and scaffold based on newly devised multilayering and mixing electrospinning techniques. *Biomaterials*, *26*(1), 37–46.

[84] **Liang, D., Hsiao, B. S., & Chu, B.** (2007). Functional electrospun nanofibrous scaffolds for biomedical applications. *Advanced drug delivery reviews*, *59*(14), 1392–1412.

[85] **Sill, T. J., & Recum, H. A.** (2008). Electrospinning: applications in drug delivery and tissue engineering. *Biomaterials*, *29*(13), 1989–2006.

[86] **Chong, E. J., Phan, T. T., Lim, I. J., Zhang, Y. Z., Bay, B. H., Ramakrishna, S., & Lim, C. T.** (2007). Evaluation of electrospun PCL/gelatin nanofibrous scaffold for wound healing and layered dermal reconstitution. *Acta Biomaterialia*, *3*(3), 321–330.

[87] **Li, D., & Xia, Y.** (2004). Electrospinning of Nanofibers: Reinventing the Wheel? *Advanced Materials*, *16*(14), 1151–1170.

[88] **Haghi, A. K., & Akbari, M.** (2007). Trends in electrospinning of natural nanofibers. *physica status solidi (a)*, *204*(6), 1830–1834.

[89] **Ki, C. S., Baek, D. H., Gang, K. D., Lee, K. H., Um, I. C., & Park, Y. H.** (2005). Characterization of gelatin nanofiber prepared from gelatin–formic acid solution. *Polymer*, *46*(14), 5094–5102.

[90] **Sukigara, S., Gandhi, M., Ayutsede, J., Micklus, M., & Ko, F.** (2003). Regeneration of Bombyx mori silk by electrospinning—part 1: processing parameters and geometric properties. *Polymer*, *44*(19), 5721–5727.

[91] **Jun, Z., Youling, Y., Kehua, W., Jian, S., & Sicong, L.** (2003). Surface modification of segmented poly(ether urethane) by grafting sulfo ammonium zwitterionic monomer to improve hemocompatibilities. *Colloids and Surfaces B: Biointerfaces*, *28*(1), 1–9.

[92] **Gupta, P., Elkins, C., Long, T. E., & Wilkes, G. L.** (2005). Electrospinning of linear homopolymers of poly(methyl methacrylate): exploring relationships between fiber formation, viscosity, molecular weight and concentration in a good solvent. *Polymer*, *46*(13), 4799–4810. Retrieved from http://www.sciencedirect.com/science/article/pii/S0032386105004167

[93] **Baumgarten, P. K.** (1971). Electrostatic spinning of acrylic microfibers. *Journal of Colloid and Interface Science*, *36*(1), 71–79.

[94] **Deitzel, J. M., Kosik, W., McKnight, S. H., Tan, N. C. B., DeSimone, J. M., & Crette, S.** (2002). Electrospinning of polymer nanofibers with specific surface chemistry. *Polymer*, *43*(3), 1025–1029.

[95] **Buchko, C. J., Chen, L. C., Shen, Y., & Martin, D. C.** (1999). Processing and microstructural characterization of porous biocompatible protein polymer thin films. *Polymer*, *40*(26), 7397–7407.

[96] **Hohman, M. M., Shin, M., Rutledge, G., & Brenner, M. P.** (2001). Electrospinning and electrically forced jets. II. Applications. *Physics of Fluids*, *13*(8), 2221.

[97] **Zhang, C., Yuan, X., Wu, L., Han, Y., & Sheng, J.** (2005). Study on morphology of electrospun poly (vinyl alcohol) mats. *European Polymer Journal*, *41*, 423–432.

[98] **Pham, Q. P., Sharma, U., & Mikos, A. G.** (2006). Electrospun poly (ε-caprolactone) microfiber and multilayer nanofiber/microfiber scaffolds: characterization of scaffolds and measurement of cellular infiltration. *Biomacromolecules*, *7*, 2796–2805.

[99] **Reneker, D. H., & Chun, L.** (1996). Nanometre diameters of polymer, produced by electrospinning. *Nanotechnology*, *7*, 216–223.

[100] **Demir, M. M., Yilgor, I., Yilgor, E., & Erman, B.** (2002). Electrospinning of polyurethane fibers. *Polymer*, *43*(11), 3303–3309.

[101] **Pawlowski, K. J., Barnes, C. P., Boland, E. D., Wnek, G. E., & Bowlin, G. L.** (2004). Biomedical nanoscience: electrospinning basic concepts, applications, and classroom demonstration. *In Mater Res Soc Symp Proc* (pp. 17–28).

[102] **Yordem, O. S., Papila, M., & Menceloğlu, Y. Z.** (2008). Effects of electrospinning parameters on polyacrylonitrile nanofiber diameter: an investigation by response surface methodology. *Materials & design*, *29*, 34–44.

[103] **Yuan, X. Y., Zhang, Y. Y., Dong, C. H., & Sheng, J.** (2004). Morphology of ultrafine polysulfone fibers prepared by electrospinning. *polymer international*, *53*, 1704–1710.

[104] **Zuo, W. W., Zhu, M. F., Yang, W., Yu, H., Chen, Y. M., & Zhang, Y.** (2005). Experimental study on relationship between jet instability and formation of beaded fibers during electrospinning. *Polymer Engineering & Science*, *45*, 704–709.

[105] **Wang, X., Um, I. C., Fang, D., Okamoto, A., Hsiao, B. S., & Chu, B.** (2005). Formation of water-resistant hyaluronic acid nanofibers by blowing-assisted electro-spinning and non-toxic post treatments. *Polymer*, *46*, 4853–4867.

[106] **Jalili, R., Hosseini, S. A., & Morshed, M.** (2005). The effects of operating parameters on the morphology of electrospun polyacrilonitrile Nanofibres. *Iranian Polymer Journal*, *15*, 1074–1081.

[107] **Mit-uppatham, C., Nithitanakul, M., & Supaphol, P.** (2004). Ultrafine electrospun polyamide-6 fibers: effect of solution conditions on morphology and average fiber diameter. *Macromolecular Chemistry and Physics*, *205*, 2327–2338.

[108] **Casper, C. L., Stephens, J. S., Tassi, N. G., Chase, D. B., & Rabolt, J. F.** (2004). Controlling Surface Morphology of Electrospun Polystyrene Fibers: Effect of Humidity and Molecular Weight in the Electrospinning Process. *Macromolecules*, *37*(2), 573–578.

[109] **Liu, H., & Hsieh, Y.-L.** (2002). Ultrafine fibrous cellulose membranes from electrospinning of cellulose acetate. *Journal of Polymer Science Part B: Polymer Physics*, *40*(18), 2119–2129.

[110] **Ohkawa, K., Kim, H., Lee, K., & Yamamoto, H.** (2004). Electrospun Non-Woven Fabrics of Poly(ϵ-caprolactone) and Their Biodegradation by Pure Cultures of Soil Filamentous Fungi. *Macromolecular Symposia*, *216*(1), 301–306.

[111] **Suadiye, D.** (2014). *Synthesis And Characterization Of Poly(Acrylonitrile-co-Vinylacetat-co-Itaconic) Acid Terpolymer As Carbon Fiber Precursor*. Istanbul Technical University.

[112] **Andrady, A. L.** (2008). *Science and technology of polymer nanofibers* (pp. 56–76). John Wiley & Sons, Inc.

[113] **Barpanda, P.** (2009). *Physical and electrochemical study of halide-modified activated carbons* (pp. 18–22). ProQuest.

[114] **Romanos, J., Beckner, M., Rash, T., Firlej, L., Kuchta, B., Yu, P., & Pfeifer, P.** (2012). Nanospace engineering of KOH activated carbon. *Nanotechnology*, *23*(1), 015401.

[115] **Manocha, S.** (2002). Studies on development of porosity in carbons from different types of biowastes. *Carbon Science*, *3*(1), 1–5.

[116] **Manocha, S. M.** (2003). Porous carbons. *Sadhana*, *28*(1-2), 335–348.

[117] **Roque-Malherbe, R. M.** (2010). *The Physical Chemistry of Materials: Energy and Environmental Applications* (pp. 124–127). CRC Press.

[118] **Serp, P., & Figueiredo, J. L.** (2009). *Carbon materials for catalysis*. *(John Wiley & Sons., Ed.)* (pp. 324–350).

[119] **Unsal, C., Kalaoglu, F., Karakas, H., & Sezai Sarac, A.** (2013). Polypyrrole/Poly (acrylonitrile- co- butyl acrylate) Composite. *Advances in Polymer Technology*, *32*(S1), E784–E792.

[120] **Sandler, S., Karo, W., Bonesteel, J., & Pearce, E.** (1998). *Polymer synthesis and characterization: a laboratory manual* (pp. 98–107, 108–119). Academic Press.

[121] **De, P., Choudhury, N., & Dutta, N.** (2010). *Thermal analysis of rubbers and rubbery materials*. ISmithers Rapra.

[122] **Brunauer, S., Emmett, P. H., & Teller, E.** (1938). Adsorption of gases in multimolecular layers. *Journal of the American Chemical Society*, *60*(2), 309–319.

[123] **Bajaj, P., Sreekumar, T., & Sen, K.** (2001). Effect of reaction medium on radical copolymerization of acrylonitrile with vinyl acids. *Journal of Applied Polymer ...*, *79*(September 1999), 1640–1652.

[124] **Paiva, M. ., Kotasthane, P., Edie, D. ., & Ogale, A. .** (2003). UV stabilization route for melt-processible PAN-based carbon fibers. *Carbon*, *41*(7), 1399–1409.

[125] **Pierotti, R. A., & Rouquerol, J.** (1985). Reporting physisorption data for gas/solid systems with special reference to the determination of surface area and porosity. *Pure Appl Chem*, *57*(4), 603–619.

[126] **Yao, Z., Chen, H.-J., Qin, Y.-X., & Cao, K.** (2011). Effect of pH Value on the aqueous precipitation copolymerization of acrylonitrile and vinyl acetate. *Journal of Applied Polymer Science*, *119*(3), 1486–1491.

[127] **Bajaj, P., Sen, K., & Bahrami, S. H.** (1996). Solution polymerization of acrylonitrile with vinyl acids in dimethylformamide. *Journal of Applied Polymer Science*, *59*(10), 1539–1550.

[128] **Hideto, K., & Kohji, T.** (1997). Mechanism and kinetics of stabilization reaction of PAN and related copolymers. *Polymer*, *29*(7), 557–562.

[129] **Dalton, S., Heatley, F., & Budd, P.** (1999). Thermal stabilization of polyacrylonitrile fibres. *Polymer*, *40*(October 1998), 5531–5543.

[130] **Wangxi, Z., Jie, L., & Gang, W.** (2003). Evolution of structure and properties of PAN precursors during their conversion to carbon fibers. *Carbon*, *41*(14), 2805–2812.

CURRICULUM VITAE

Name Surname:	Sahand Faraji
Place and Date of Birth:	Tabriz 1989
Address:	Bahcekoy Ogrenci Yurdu, Hacı Osman Bayırı, İSKİ Yanı, Sarıyer, İstanbul, Turkey
E-Mail:	sahandfaraji@gmail.com
B.Sc.:	Tabriz University/ Chemical Engineering